NOTICE

The quality of this microform is heavily dependent upon the quality of the original thesis submitted for microfilming. Every effort has been made to ensure the highest quality of reproduction possible.

If pages are missing, contact the university which granted the degree.

Some pages may have indistinct print especially if the original pages were typed with a poor typewriter ribbon or if the university sent us an inferior photocopy.

Reproduction in full or in part of this microform is governed by the Canadian Copyright Act, R.S.C. 1970, c. C-30, and subsequent amendments.

AVIS

La qualité de cette microforme dépend grandement de la qualité de la thèse soumise au microfilmage. Nous avons tout fait pour assurer une qualité supérieure de reproduction.

S'il manque des pages, veuillez communiquer avec l'université qui a conféré le grade.

La qualité d'impression de certaines pages peut laisser à désirer, surtout si les pages originales ont été dactylographiées à l'aide d'un ruban usé ou si l'université nous a fait parvenir une photocopie de qualité inférieure.

La reproduction, même partielle, de cette microforme est soumise à la Loi canadienne sur le droit d'auteur, SRC 1970, c. C-30, et ses amendements subséquents.

ISBN 0-315-53296-3

STUDY OF IMPEDANCE STEP AND INDUCTIVE STRIP OF FINLINE

by

YIN-LAN TSUI, B.A.Sc.

A thesis submitted to the
School of Graduate Studies and Research
in partial fulfillment of the requirements
for the Degree of
Master of Applied Science

Ottawa-Carleton Institute for Electrical Engineering
The Department of Electrical Engineering
Faculty of Engineering
University of Ottawa

ACKNOWLEDGEMENTS

The author wishes to express her most sincere gratitude to her supervisor, Dr. W.J.R. Hoefer, for his valuable advice and guidance throughout this work.

The author is particularly grateful to Miss E.K. Chan and Mr. W. Yue for their support and Tex format in this text.

The author would like to thank her husband for his understanding and support throughout this thesis.

Finally, special thanks are given to the sisters for their encouragement and never failing confidence in the author.

ABSTRACT

New closed-form expressions for the parameters of impedance steps and inductive strips in unilateral finlines are presented. They are empirical formulae based on equivalent circuits of the discontinuities and their spectral domain analysis. The expressions are adequate for most practical finline circuit design projects and well suited for computer aided design (CAD). Finline circuits find increasing applications in millimeter-wave communication and radar systems operating in the 18 to 140 GHz range.

CONTENTS

LIST OF TABLES

LIST OF FIGURES

CHAPTER 1

INTRODUCTION

Finline is a promising transmission medium at microwave frequencies above 20 GHz. Meier [1] was the pioneer who proposed the integrated finline technology. Throughout the years, many applications of finlines have been reported in the literature. Some particularly successful applications of finline design are PIN-attenuators [1], filters [2], balanced mixers [3], power dividers [4] and oscillators [5].

The evaluation of the guided wavelength (or, alternatively, the effective dielectric constant) and characteristic impedance in finline has been presented by Meier [1], Hofmann [2], Saad and Begemann [6], Chang and Itoh [7], and Hoefer [8]. Most of these methods are very complex, involving sophisticated computer programming or precision measurements (as in Meier's procedure [1]). An alternative to these complicated methods is to derive closed-form expressions. This approach has been presented by Pramanick and Bhartia [9].

1.1 ADVANTAGES OF FINLINE OVER WAVEGUIDE AND MICROSTRIP

In the past, waveguide was the exclusive transmission medium for millimeter-waves. Its low conduction and zero radiation losses, and its high power handling capability are very attractive for transmission of millimeter-waves. However, the manufacturing of waveguide components is expensive and not well suited for production in large quantities. Microstrip has replaced the waveguide in numerous applications at frequencies up to 30 GHz, and has shown potential up to 140 GHz. Its low cost and its suitability for mass production with batch processing techniques make it a superior choice over waveguide in many applications. However, when microstrip is operated above 30 GHz, it becomes quite lossy and small in size.

For operating frequencies above 30 GHz, finline is a better technology in many aspects. It is almost as easy to fabricate as microstrip, is compatible with semiconductor devices, has a wide single-mode bandwidth, moderate attenuation and low dispersion. One of the major issues that must be addressed before widespread application of finlines becomes possible, is the characterization of finline discontinuities. Simple but accurate models for discontinuities are essential for successful design and realization of finline circuits. This study therefore deals with the two most frequently encountered discontinuities, namely the impedance step and the symmetrical inductive strip.

1.2 MOTIVATION AND PURPOSE OF STUDY

Since the basic building blocks of finline circuits are the discontinuities, there is a great

need to analyse them accurately. The most successful numerical technique used to analyse finline discontinuities are the spectral domain technique, the mode-matching technique, and the transmission line matrix method. Among them, the spectral domain technique combined with the mode-matching technique seem to be the most popular.

Pic and Hoefer [17] have determined the characteristics of inductive strips and impedance steps by measuring the resonant frequencies of a rectangular cavity containing them. Meanwhile, Sorrentino and Itoh [12] have evaluated the resonant frequencies of a finline resonator containing a step discontinuity with the transverse resonance technique.

On the other hand, Helard et al [15] computed the coupling coefficients between eigenmodes at a step discontinuity in unilateral finline with a thorough spectral domain approach. Koster and Jansen [11] utilized the hybrid-mode spectral domain approach to investigate the scattering matrices of symmetric and asymmetric inductive strip discontinuities in unilateral finlines. Finally El-Hennawy and Schuenemann [14] analysed step discontinuities, inductive notches, small capacitive strips, and longitudinal strips for mounting a semiconductor device, with the mode-matching technique.

Numerical techniques are highly accurate methods and powerful tools for analysing discontinuities. However, they always require considerable analytical effort and involve complicated computer programming. Furthermore, the time required for one computation is far too long for their implementation in an interactive CAD procedure, let alone an optimization involving a large number of analyses. For this reason, closed-form expressions for the characteristics of discontinuities are much more effective for the design, provided that they are sufficiently accurate and cover a broad range of geometries.

1.3 IMPORTANCE OF COMPUTER-AIDED DESIGN (CAD)

The conventional procedure for the design of microwave circuits is outlined in Fig. 1.1 [20]. One starts with the circuit specifications and arrives at an initial circuit design. Available design data and experience are helpful in forming the initial circuit configuration. Analysis and synthesis procedures are used for determining the values of various circuit parameters. Once these parameters are found, a first laboratory model is built for initial testing. Measurements of the laboratory model are made to evaluate its characteristics. Finally, the measured results are compared with the initial circuit specifications.

If the initial specifications are not met, modifications of the circuit are carried out in the form of adjustments, tuning, and trimming of the circuit. The modified model is then subjected to further measurements and comparison with the initial specifications. The sequence of modifications, measurements and comparison is repeated until the initial specifications are met. Sometimes, the specifications are compromised if it turns out that the circuit cannot meet them. Once the final circuit configuration is determined, it can be passed on for fabrication of a prototype and subsequent production.

The above procedure has been used in the design of microwave circuits for quite some time. However, it has become increasingly difficult to use this iterative and empirical method successfully because of the following considerations:

i) Increased complexity of modern systems demands more precise and accurate design of circuits and subsystems. Therefore, tolerances in the circuit design must be observed very closely.

ii) A large variety of passive and active components is available for realizing microwave

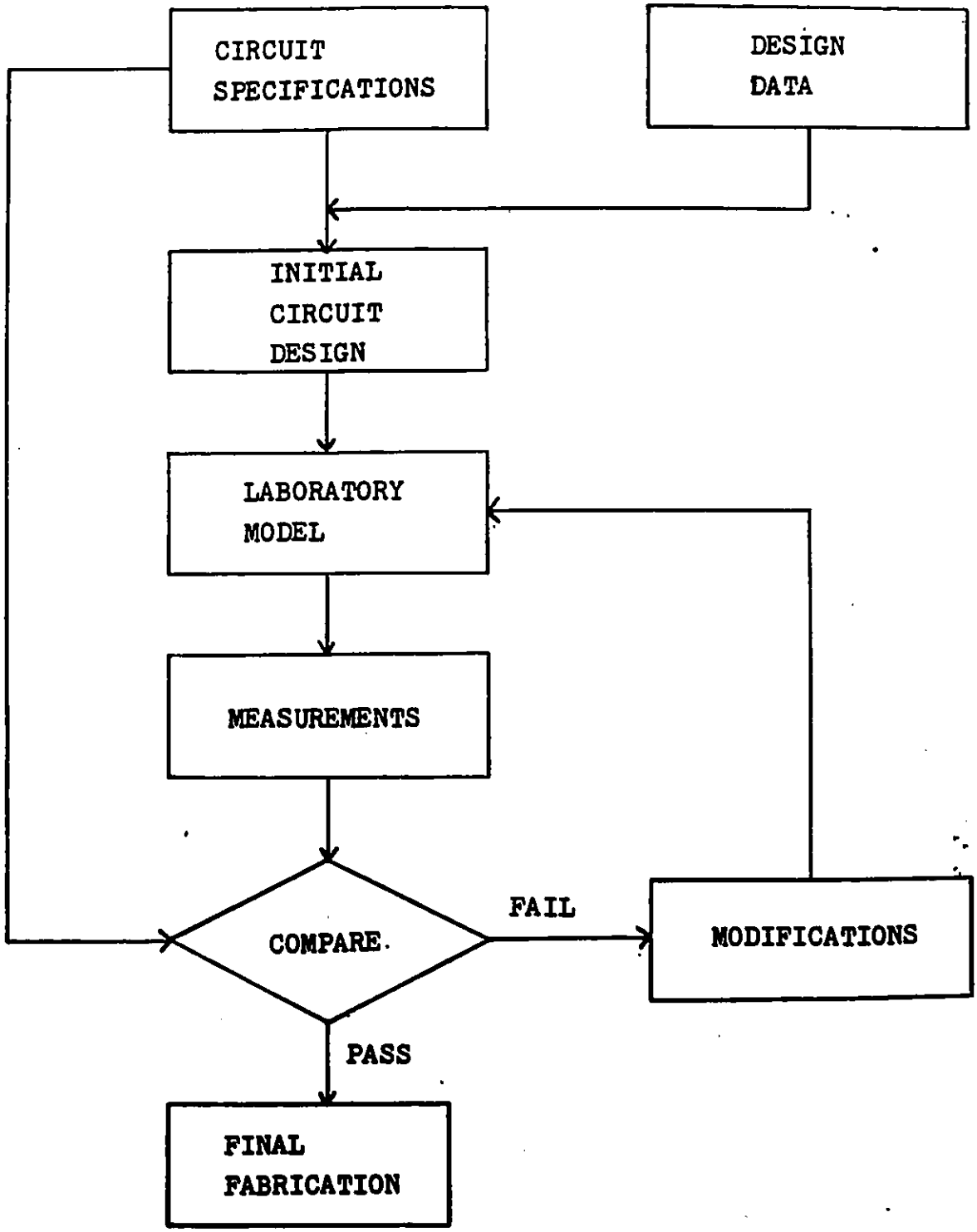

Figure 1.1 Conventional procedure for microwave circuit design.

circuits. It would be uneconomical to select the most appropriate components by building a large number of experimental laboratory models.

iii) If MIC technology is used to build the laboratory model, it is very difficult or impossible to modify a circuit. Furthermore, the design and fabrication cycles are very long (often several weeks).

In order to avoid these problems, "computer aided design" (CAD) techniques are used for circuit design. Actually, the competitive design of most microwave integrated circuits would be impossible without CAD facilities.

A typical flow diagram for a CAD procedure is shown in Fig. 1.2 [20]. The synthesis methods and available design data are stored in computer memory. This pre-stored information is useful in designing the initial circuit. The performance of this initial circuit is then evaluated by a circuit analysis package. The equivalent circuits and the corresponding parameters of various components (passive and active) are stored in files or subroutines, which are called by the main routine.

The performance of the initial circuit is compared with the given specifications. If these specifications are not met, then the variable parameters of the circuit are altered in a systematic manner. This procedure called optimization, includes sensitivity analysis of the circuit which calculates changes in the circuit parameters. The sequence of circuit analysis, comparison with the given specifications and the modifications is performed iteratively until the specifications are met or the optimum performance of the circuit (within the given constraints) is reached.

After the optimization of the circuit parameters, a prototype is fabricated, and measurements are made to compare its performance with the given specifications. Some modifications may still be needed if the modelling of the components during the analysis was not accurate

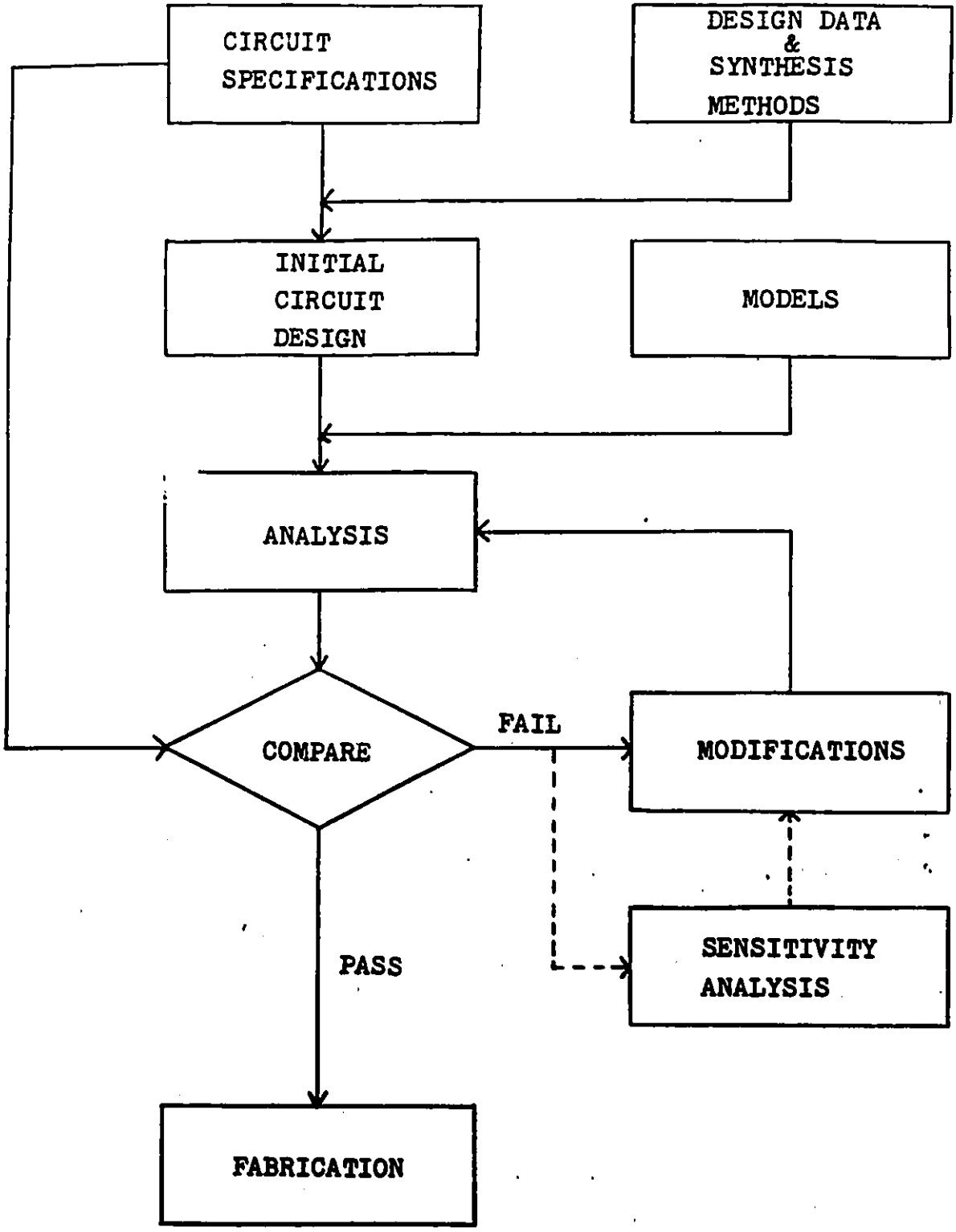

Figure 1.2 CAD procedure for microwave circuit design.

enough. However, in these final phase, these modifications will usually be small compared with those required in the conventional circuit design procedure. Typically, the time required for the successful design and realization of a prototype is reduced by one order of magnitude through the use of CAD procedures.

In conclusion, the process of CAD, as outlined above, consists of three important segments, namely:

i) Modelling

ii) Analysis, and

iii) Optimization.

Its success depends critically on the availability of simple and accurate models for the various circuit components. Its application leads to the following advantages over the conventional design process:

i) It reduces the necessary development time,

ii) It has a higher potential for alternative solutions due to easy simulation, and thus shortens reaction times,

iii) It can use already existing designs and modify them easily to meet new specifications.

The aim of this thesis is to make a contribution to the development of reliable models for the CAD of finline circuits.

CHAPTER 2

BASIC THEORY AND DESCRIPTION OF DISCONTINUITIES

2.1 THE EFFECT OF DISCONTINUITIES ON THE DOMINANT MODE IN RECTANGULAR WAVEGUIDE

In rectangular waveguide, the dominant propagating mode is the TE_{10} mode. In the large marjority of applications, single mode propagation is desirable to maintain a predictable field distribution and avoid losses due to mode conversion. Therefore, the waveguide is used in the recommended operating range of frequencies.

When an obstacle is present in a waveguide, higher order modes are excited by it. These modes are evanescent as long as the operating frequency is below their cutoff frequency. They decay exponentially in both directions from the obstacle which excites them. Thus, the fringing field around the obstacle is practically localized.

The evanescent modes are excited by an obstacle to satisfy the required boundary conditions: the tangential electrical field must be zero, and the tangential magnetic field must be maximum on the obstacle (if it is conducting). The non-propagating modes store reactive energy. When the reactive energy is predominantly magnetic, the obstacle will behave as an

inductivity. On the other hand, if the stored energy is mainly electric, then the obstacle is capacitive. Fig. 2.1 shows some shunt inductive elements, whereas Fig. 2.2 shows some examples of shunt capacitive elements in a waveguide. The stored reactive energy determines the amplitude and phase of the reflected dominant wave and simulates the presence of an equivalent inductance or capacitance in the waveguide.

The reference plane for determining the impedance of a discontinuity must be sufficiently far away from the obstacle so that the fields in this plane are only those of the incident and reflected dominant waves, and the higher order fields have decayed to a negligible value. This is also important in any experimental setup used to measure the impedance of a particular discontinuity.

Once the impedance of a discontinuity in a reference plane is obtained, it can be transformed to any other plane, for example, to a plane that is located near the discontinuity, by using the following impedance-transformation formula:

$$Z(L_2) = Z_c \frac{Z(L_1) + jZ_c tan\beta(L_2 - L_1)}{Z_c + jZ(L_1) tan\beta(L_2 - L_1)} \tag{2.1}$$

where,

L_1 = location of the reference plane

L_2 = location of the transformed plane

β = phase constant of the waveguide

Z_c = characteristic impedance of the guide

$Z(L_1)$ = impedance function at plane located at L_1

$Z(L_2)$ = impedance function at plane located at L_2.

Thus, the impedance in the plane that contains the discontinuity can be obtained by using equation (2.1) as long as the impedance at a plane far away from the discontinuity is known.

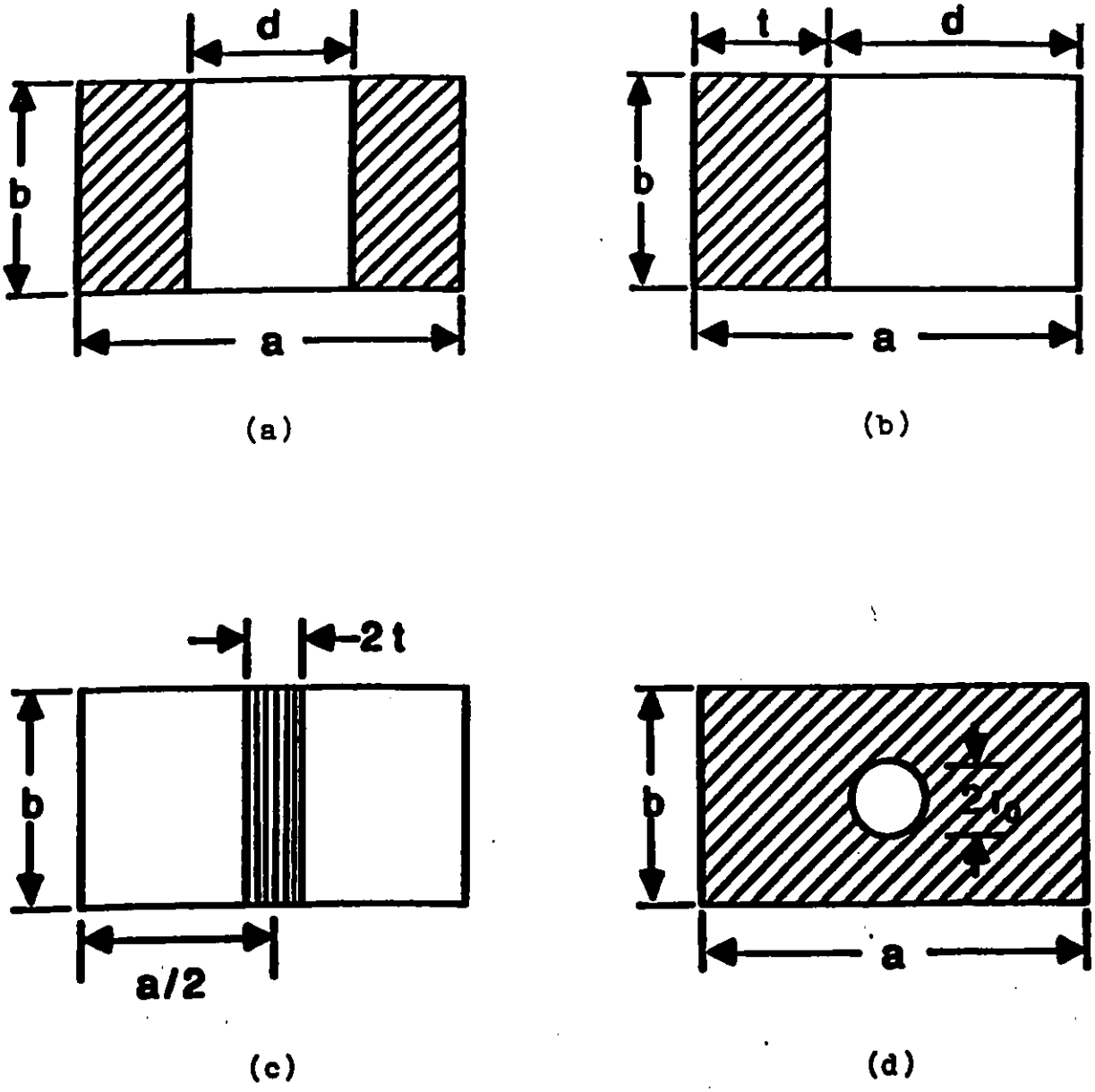

Figure 2.1 Shunt inductive elements. (a) Symmetrical diaphragm; (b) asymmetrical diaphragm; (c) thin circular post; (d) small circular aperture.

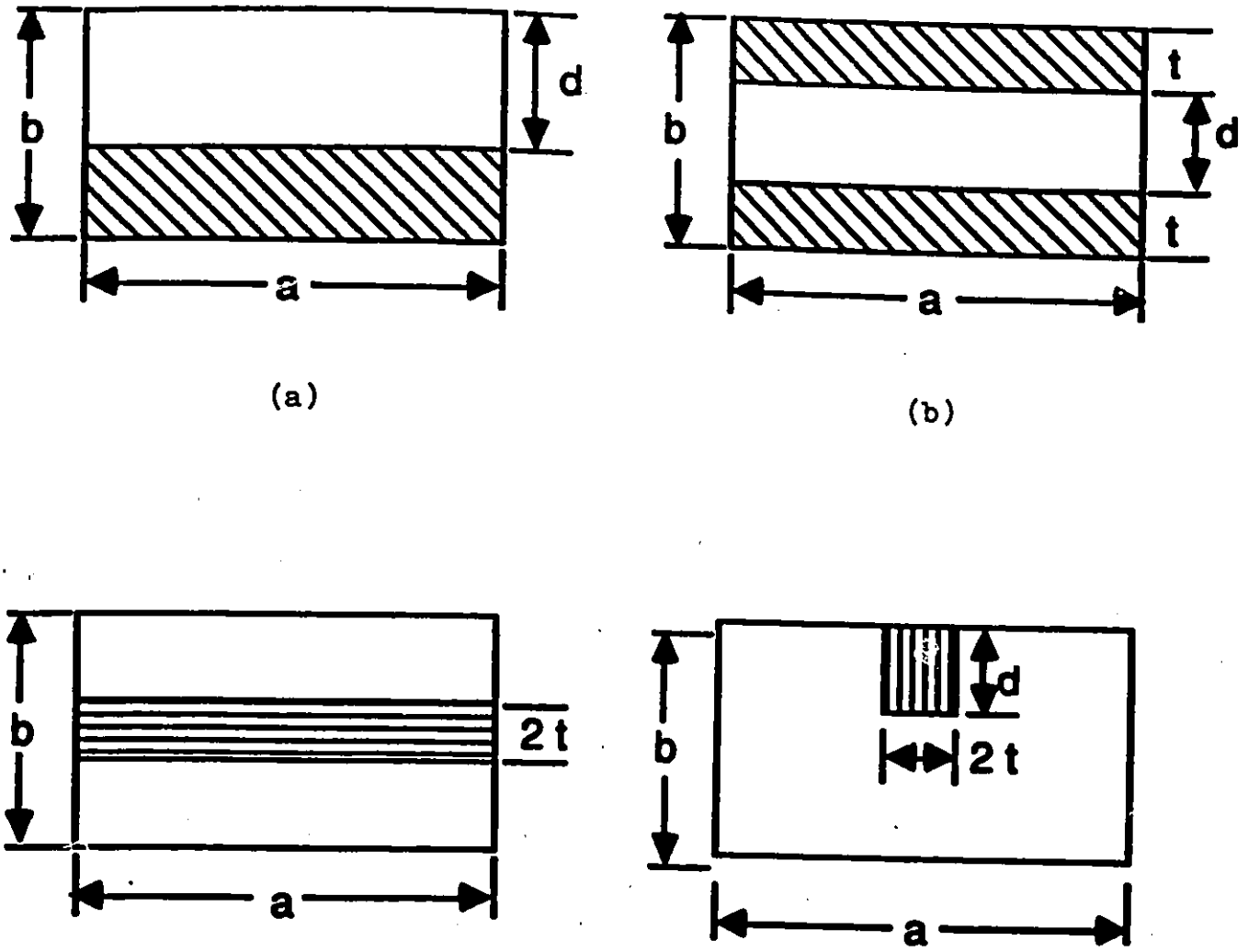

Figure 2.2 Shunt capacitive elements. (a) Asymmetrical capacitive diaphragm; (b) symmetrical diaphragm; (c) capacitive rod; (d) capacitive post.

But one must always keep in mind that the impedance at the plane that is located in the vicinity of an obstacle describes the effect of the obstacle on the dominant mode only. It does not imply that the total field at this particular reference plane is that of the dominant mode only. Moreover, the detailed field structure near the obstacle is not revealed by the impedance function at this location. Nevertheless, the detailed field structure at the obstacle is rarely required.

2.2 DISCONTINUITIES IN MICROSTRIP

Any design of microstrip circuits requires characterization of various discontinuities. Since discontinuity dimensions are usually much smaller than the wavelength in microstrip, they may be approximated by lumped element equivalent circuits. However, a more complete characterization involves determination of frequency-dependent scattering coefficients associated with the discontinuity. It is much more important to characterize discontinuities in microstrip circuits accurately than in coaxial lines and waveguides. The reason is that the microstrip circuits do not lend themselves to easy adjustments or tuning after fabrication. If a provision is made for adjustments, the main advantages of compactness and reliability gained by the use of microstrip circuits are lost (at least partially).

A discontinuity in microstrip is caused by an abrupt change in the geometry of the strip conductor. Electric and magnetic field distributions are modified near the discontinuity. The altered electric field distribution gives rise to a change in capacitance, and the changed magnetic field distribution can be represented by an equivalent inductance. Thus, the analysis of microstrip discontinuities involves the evaluation of these capacitances and inductances.

Analysis of microstrip discontinuities can either be based on quasi-static considerations, or carried out more rigorously by fullwave analysis. Quasi-static methods assume that the mode of propagation is purely TEM. In that case, discontinuity characteristics are calculated from the static capacitance or inductance of the structure, and equivalent circuits for discontinuities may be derived from these results. This analysis is adequate for designing circuits at lower frequencies where the strip width and the substrate thickness are much smaller than the wavelength in the dielectric material.

Another analysis method is a waveguide type dynamic analysis taking dispersion and higher order modes into account. A dispersion model is set up first. The deviation from the TEM nature is accounted for quasi-empirically. Some parameters of the model are determined such that they agree with the known experimental (or exact theoretical) dispersion behavior of the microstrip. This leads to a frequency-dependent scattering matrix of the discontinuity. Equivalent circuits for discontinuities with frequency-dependent elements can be based on these results.

On the other hand, a fullwave analysis can be carried out to analyse microstrip structures. This is the most rigorous approach among the three. Since the actual modes are hybrid modes, i.e. a superposition of TE and TM fields, longitudinal components of both the electric and magnetic fields are present. Therefore, the hybrid modes supported by the microstrip cannot be fully described in terms of static capacitances and inductances; one has to introduce time-varying electric and magnetic fields and solve the wave equation, which yields the mode propagation constants directly. Fig. 2.3 illustrates the differences between the quasi-static and the hybrid field distribution in a microstrip line. The presence of longitudinal field components is clearly visible in the hybrid case. Discontinuity parameters are then calculated by determining the hybrid field distribution at the discontinuity [26] and [29].

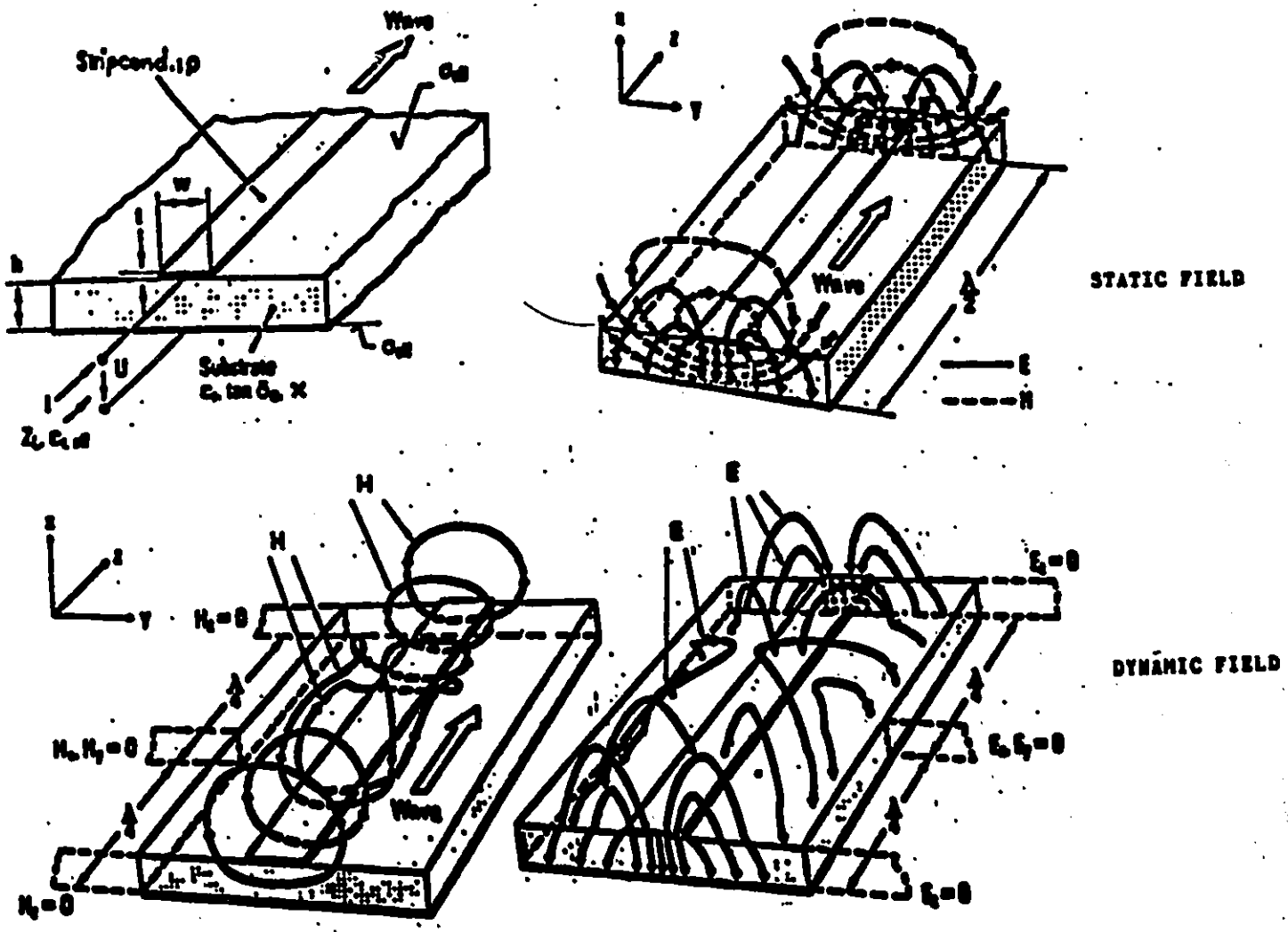

Figure 2.3 Quasi-static and hybrid field distribution in a microstrip line [26].

2.3 DISCONTINUITIES IN FINLINE

As in waveguide and microstrip, evanescent modes arise in a finline wherever there is an obstacle, such as an abrupt change in the geometry of the substrate, in the path of transmission. However, it is more difficult to analyse the discontinuities in finline than that in waveguide and microstrip. The reason is that the non-TEM nature of propagation in finline renders quasi-static analysis impossible. Furthermore, the conventional methods of analysing waveguide discontinuities cannot be applied on finline due to its inhomogeneity. Thus, numerical methods are most commonly employed to analyse finline structures. Closed-form expressions of two important finline devices are developed in this thesis. Their applications are discussed below.

2.4 APPLICATIONS OF FINLINE IMPEDANCE STEPS

Impedance steps are essentially used for impedance transformation. One important application of such steps is the realization of transitions between waveguide and finline.

Such a transition can either be a taper or multi-step impedance transformer. Their basic building block is an impedance step as shown in Fig. 2.4. A smooth taper can be decomposed into a large number of infinitesimal impedance steps and analysed for the limit of zero step length [22]. Fig. 2.5 shows a multi-step impedance transformer realized in a back-to-back configuration for easy measurement. The number of steps determines the bandwidth of the transition, and depends on the impedance ratio it is designed to overcome. The availability of a closed-form expression for a single impedance step permits the designer to analyse and design both types of transitions with a minimum of computations. The small difference between the

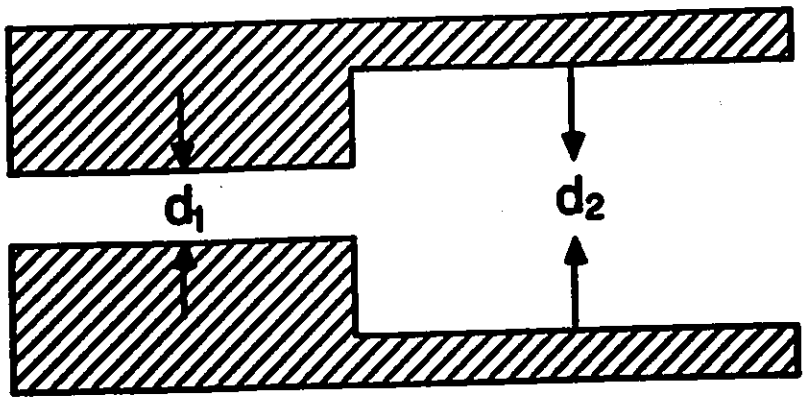

Figure 2.4 An impedance step.

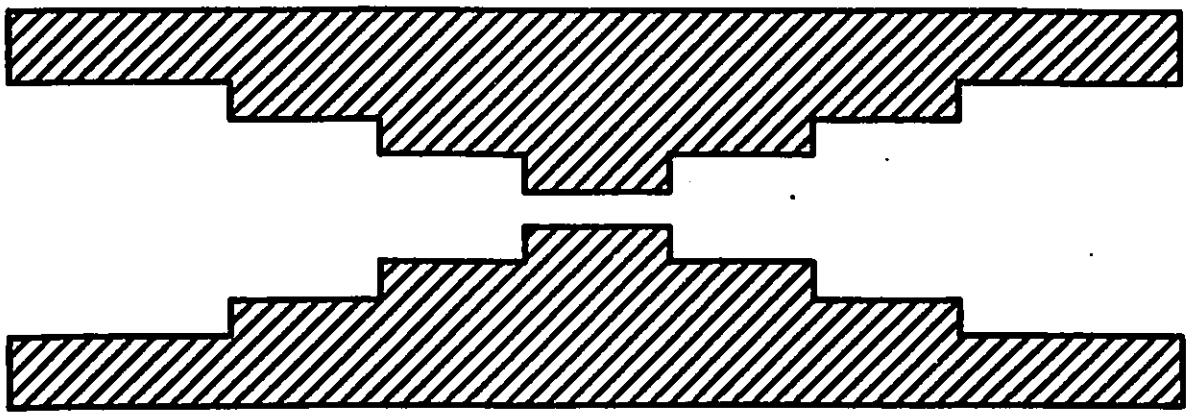

Figure 2.5 A multi-step impedance transformer.

results obtained with highly sophisticated numerical methods and the method proposed here is acceptable for most practical design purposes. However, the gain in simplicity and convenience yielded by the use of closed-form expressions is considerable. The derivation of the empirical formulae for step discontinuities is described in Chapter 3.

2.5 APPLICATIONS OF INDUCTIVE STRIPS IN FINLINE

Inductive strips act as shunt inductances and can therefore be used to realize Chebyshev-type bandpass filters (similar to post-coupled waveguide filters). A bandpass filter is used to provide as nearly perfect transmission as possible for signals falling within desired passband frequency ranges, together with rejection of those signals and noise outside the desired frequency bands. In addition, it can perform as an ideal broadband impedance-matching structure which will cut off sharply at the edges of the band of impedance match for almost all types of loads. Again, the availability of a simple closed-form model for inductive strips greatly simplifies the design and analysis of such filter structures.

Fig. 2.6 shows one possible structure of a bandpass filter. It is an end-coupled resonator filter consisting of $\frac{\lambda}{2}$ resonators. Thus, the basic building block of a bandpass filter is indeed an inductive strip as shown in Fig. 2.7. As in the case of an impedance step, there are numerous rigorous analytical methods available to investigate the inductive strip. The closed-form model presented in this thesis is satisfactory for medium- and broad-band filter design, and only narrow band filters require more accurate numerical treatment which account for higher-order mode interaction between neighboring strips. The derivation of the closed-form expressions for transverse inductive strips is described in Chapter 4.

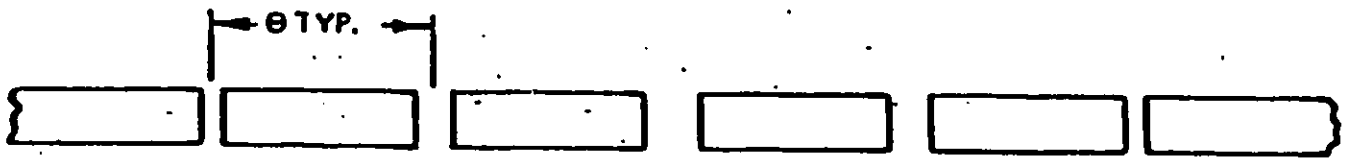

Figure 2.6 Basic configuration for end-coupled resonator bandpass filter.

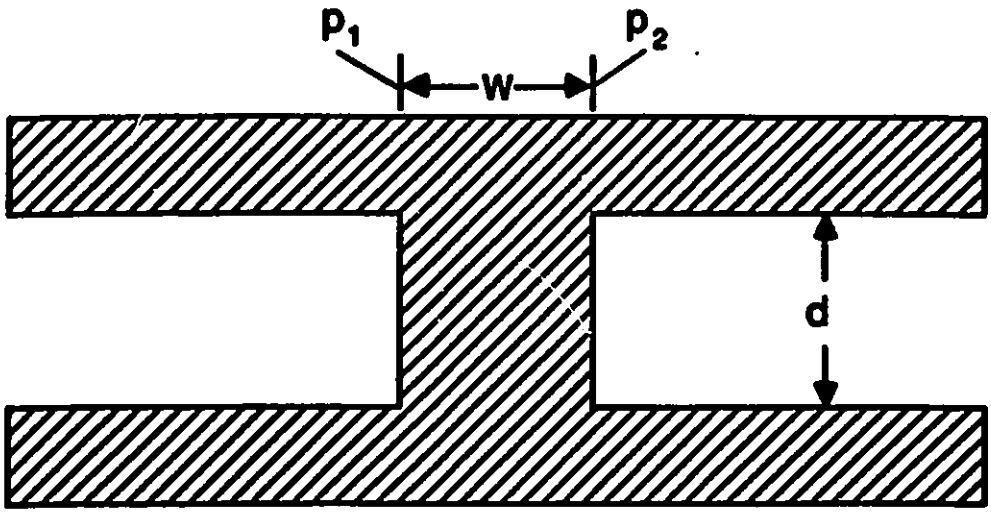

Figure 2.7 An inductive strip.

CHAPTER 3

THE DERIVATION AND ACCURACY OF EMPIRICAL FORMULAE OF AN IMPEDANCE STEP

3.1 EQUIVALENT CIRCUIT OF A STEP IMPEDANCE

As mentioned in Section 2.4, an impedance step is a basic building block of an impedance transformer. Fig. 3.1 shows an impedance step and its equivalent circuit. Z_1 represents the characteristic impedance (Power-Voltage definition) of the narrow part of the step, whereas Z_2 represents the characteristic impedance of the wider part. It is important to note that the transformer ratio of the step cannot be obtained simply by evaluating the ratio of the characteristic impedances of each line section computed separately. For example, when d_1=0.25mm, d_2=0.85mm, and when all other dimensions are as shown in Fig. 3.2, the characteristic impedances (using the spectral domain technique) are :

at	d_1=0.25mm	Z_1(V,P)=146.99Ω
	d_2=0.85mm	Z_2(V,P)=259.32Ω

and their ratio is:

$$\frac{Z_2(V,P)}{Z_1(V,P)} = 1.764$$

However, when using the empirical formulae which will be derived in Section 3.3,the trans-

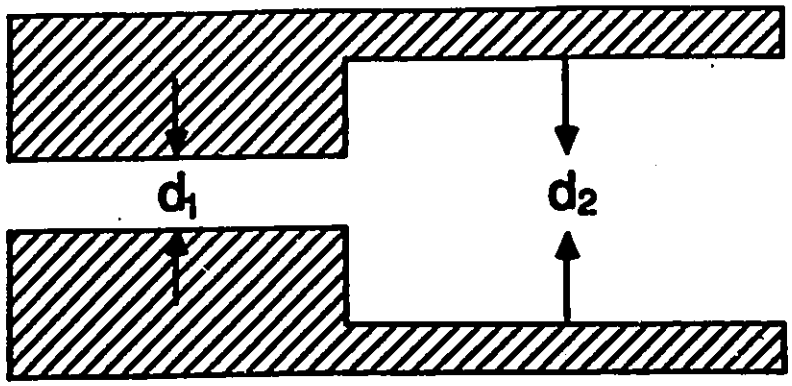

(a)

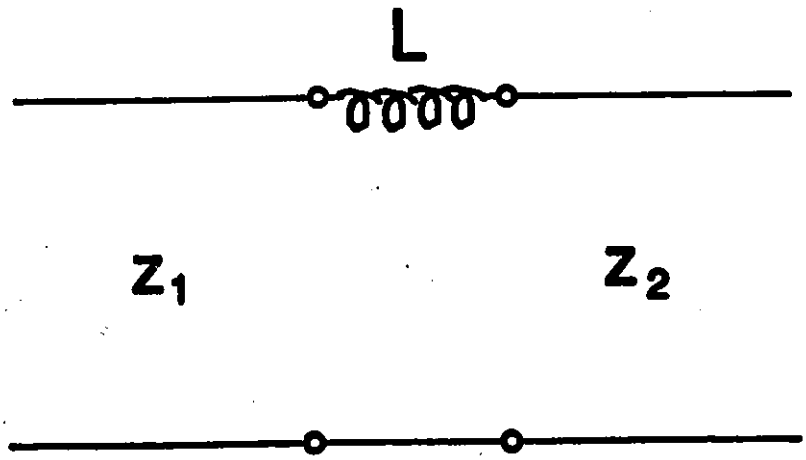

(b)

Figure 3.1 A step impedance and its equivalent circuit.

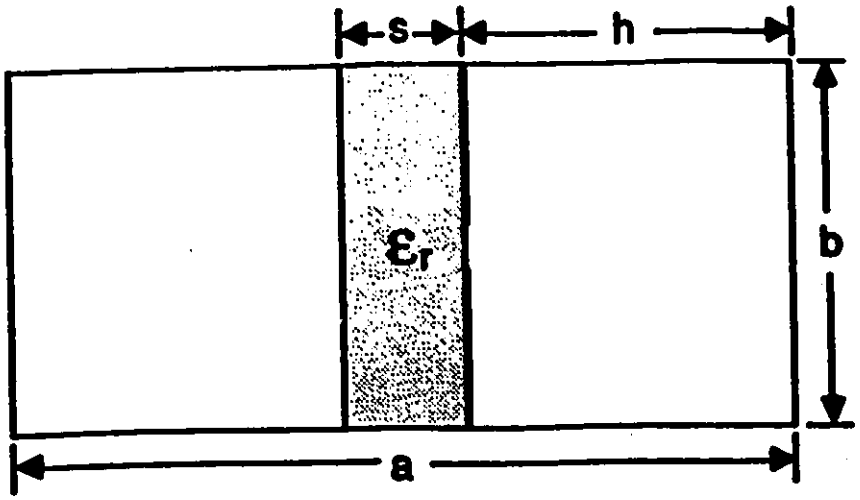

Figure 3.2(a) A cross-section of a unilateral finline.

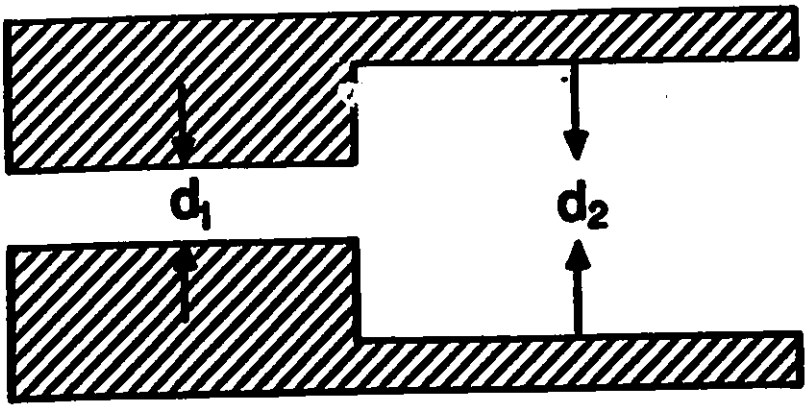

Figure 3.2(b) A step impedance.

a=7.112mm, b=3.556mm, s=0.254mm, h=3.429mm,

d_1=0.25mm, d_2=0.85mm, ε_r=2.22, f=35GHz

former ratio ρ is found as ρ=1.714. In effect, the difference between these two results is

$$\Delta = \frac{1.764 - 1.714}{1.714} \approx 3\%$$

The inductance L in the equivalent circuit accounts for the magnetic energy stored by the discontinuity. The current lines shown in Fig. 3.3 show that the fin current must travel an excess distance from the narrow part to the wider part of the step. This indicates that the step introduces a small excess length in the line, which is equivalent to a series inductance L. Other equivalent circuit models have been proposed by El-Hennawy[14], Pic and Hoefer[17], and Helard et al [22]. However, the equivalent circuit shown in Fig. 3.1 lends itself to an easy formulation over a broad frequency band in the form of an analytical expression.

3.2 THE S-PARAMETERS OF AN IMPEDANCE STEP

S-parameters are commonly employed to describe microwave circuit components because they can be measured easily. The S-parameter measurements are carried out by terminating all ports with their normalizing impedance. Quantities such as the reflection coefficient and the transmission coefficient can be expressed directly in terms of the scattering parameters.

Another important advantage of the S-matrix approach emerges from the fact that the S-parameters are defined on the basis of traveling waves and, unlike terminal currents or voltages, the wave amplitudes do not vary in magnitude along a lossless line. This allows the S-parameters for an unknown device to be measured relatively far away from its physical location. The effect of the shift of the reference plane along a length of lossless line may be accounted for by modifying the phase of the measured data.

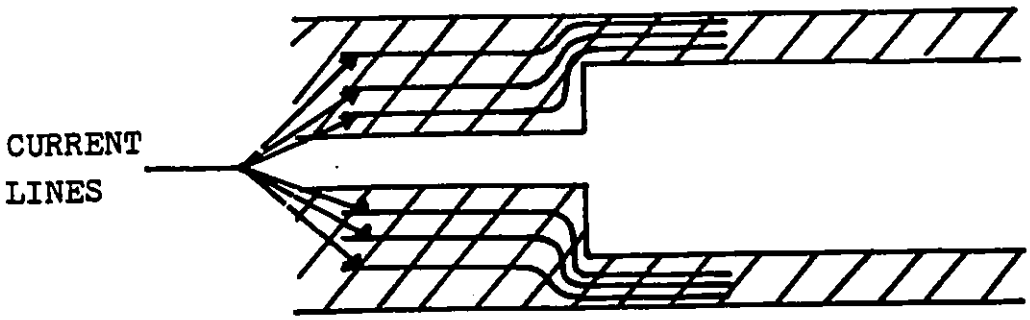

Figure 3.3 A step impedance showing the extra path length travels by the fin current.

Using the symbols of the equivalent circuit parameters in Fig. 3.1, the scattering parameters of the impedance step are found as:

$$S_{11} = \frac{\frac{Z_2}{Z_1} - 1 + j\frac{\omega L}{Z_1}}{\frac{Z_2}{Z_1} + 1 + j\frac{\omega L}{Z_1}} \tag{3.1}$$

$$S_{22} = \frac{\frac{-Z_2}{Z_1} + 1 + j\frac{\omega L}{Z_1}}{\frac{Z_2}{Z_1} + 1 + j\frac{\omega L}{Z_1}} \tag{3.2}$$

$$S_{12} = \frac{2\sqrt{\frac{Z_2}{Z_1}}}{\frac{Z_2}{Z_1} + 1 + j\frac{\omega L}{Z_1}} \tag{3.3}$$

$$S_{21} = S_{12} \tag{3.4}$$

Equation (3.4) applies since an impedance step is a reciprocal network.

The S-parameters in equations (3.1) to (3.4) are evaluated by choosing the equivalent voltages in such a way that the power is given by $\frac{1}{2}\frac{|V_n|^2}{Z_0}$ for all modes. V_n is the voltage wave traveling in the positive z-direction at the nth port. The main reason for doing this is to obtain a symmetrical scattering matrix for reciprocal structures. If this normalization is not used, then because of different impedance levels in different lines, the scattering matrix cannot be symmetrical. The closed-form expressions for the equivalent circuit parameters are derived in Section 3.3. A case study of an impedance step can be found in Appendix A.

3.3 THE DERIVATION OF EMPIRICAL FORMULAE FOR AN IMPEDANCE STEP

Schmidt [16] has computed the S-parameters of an impedance step in the Ka band for various step widths. Fig. 3.4[16]shows the S-parameters in Ka band with d_1=0.25mm and

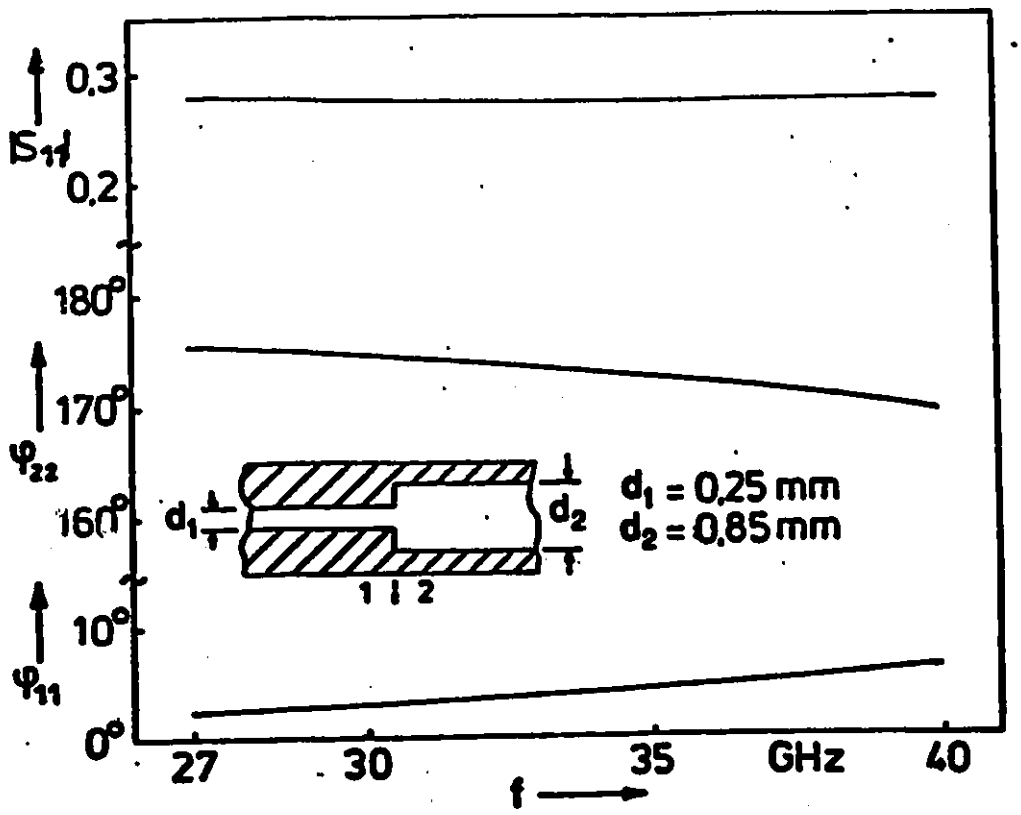

Figure 3.4 The S-parameters of a step impedance at Ka band.

d_2=0.85mm. Fig. 3.5[16]shows the S-parameters for various step width ratios with d_1=0.25mm where d_2 varies from 0.25mm to 3.6mm, at 35 GHz.

From equations (3.1) and (3.2):

$$S_{11} = \frac{\frac{Z_2}{Z_1} - 1 + j\frac{\omega L}{Z_1}}{\frac{Z_2}{Z_1} + 1 + j\frac{\omega L}{Z_1}} \tag{3.1}$$

$$S_{22} = \frac{\frac{-Z_2}{Z_1} + 1 + j\frac{\omega L}{Z_1}}{\frac{Z_2}{Z_1} + 1 + j\frac{\omega L}{Z_1}} \tag{3.2}$$

Replacing $\frac{Z_2}{Z_1}$ by x and $\frac{\omega L}{Z_1}$ by y, equations (3.1) and (3.2) can be rewritten as

$$S_{11} = \mid S_{11} \mid e^{j\varphi_{11}} = \frac{x - 1 + jy}{x + 1 + jy} \tag{3.5}$$

$$S_{22} = \mid S_{22} \mid e^{j\varphi_{22}} = \frac{-x + 1 + jy}{x + 1 + jy} \, . \tag{3.6}$$

Applying the reciprocity and lossless conditions we have

$$\mid S_{22} \mid = \mid S_{11} \mid \, . \tag{3.7}$$

Thus, we have two unknowns: x and y in two linear equations. Thus, x and y can be solved for if S_{11} and S_{22} are known.Indeed, $\mid S_{11} \mid$, φ_{11} and φ_{22} can be taken from Fig. 3.5 at various values of d_2. (We have chosen values of d_2 at regular intervals of 0.2 mm.) x and y are then solved for those particular d_2 values.

Utilizing Pramanick's equations in [9] to obtain Z_1 for various d_2, the inductance L can be found as a function of d_2, or better still as a function of $\frac{d_2}{d_1}$. Values of $\frac{Z_2}{Z_1}$ and L for various $\frac{d_2}{d_1}$ ratio, are interpolated and plotted in Fig. 3.6 and Fig. 3.7, respectively. Fitting a smooth curve through these sample points yields the following empirical formulae [25] for $\frac{Z_2}{Z_1}$ and L:

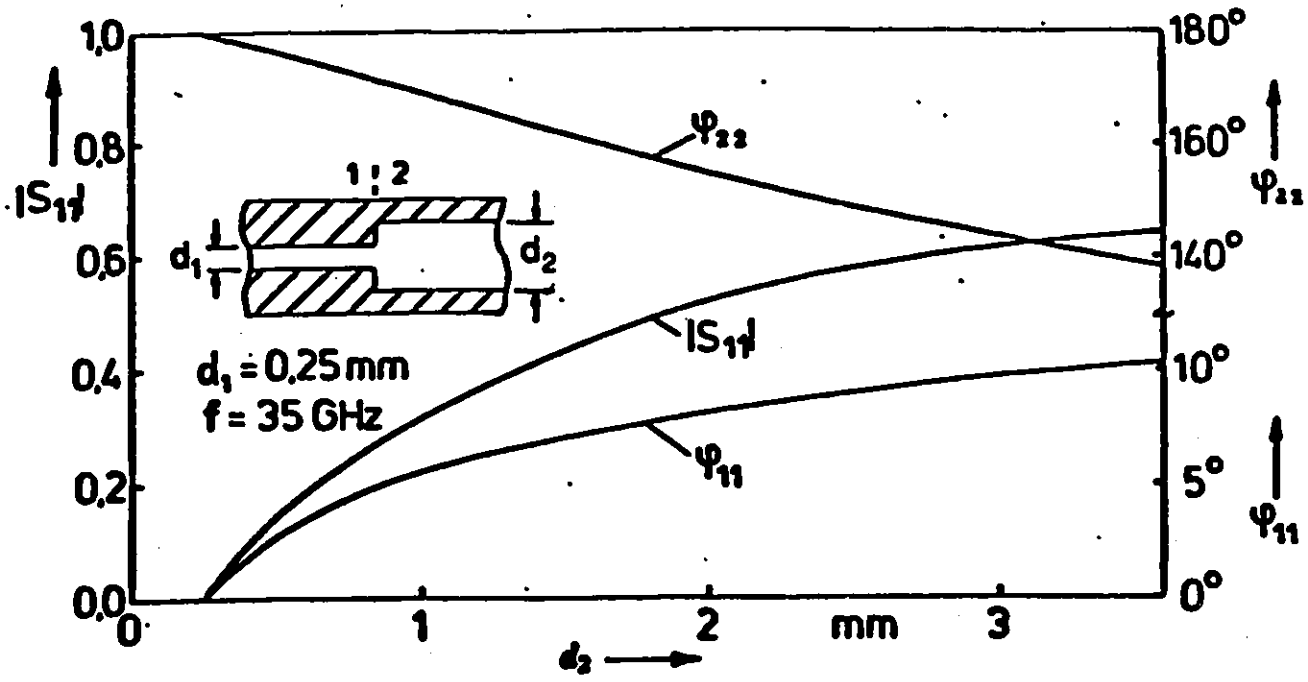

Figure 3.5 The S-parameters of a step impedance with the wider step varies in step width.

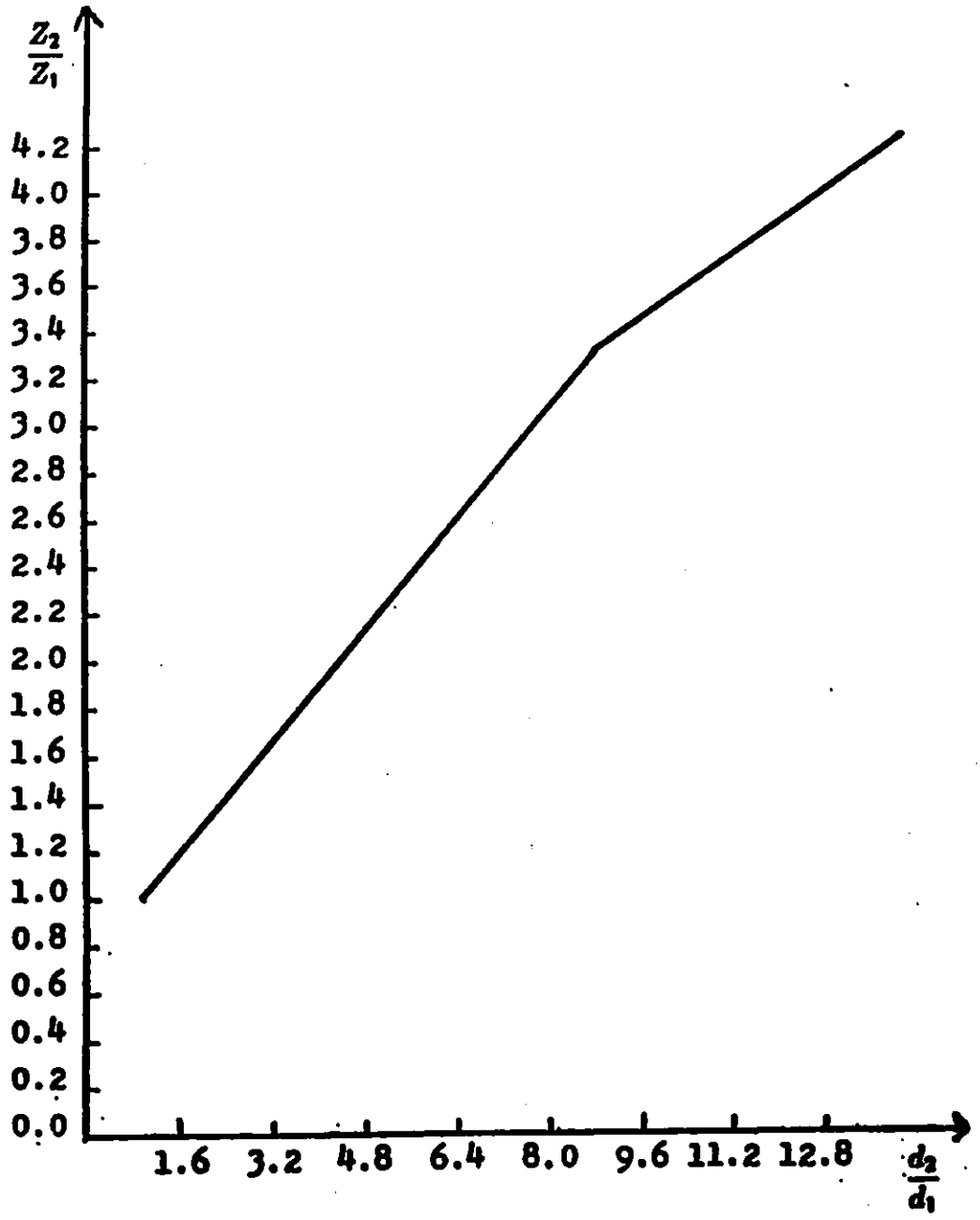

Figure 3.6 The impedance ratio of an impedance step as a function of the step width ratio in the Ka band.

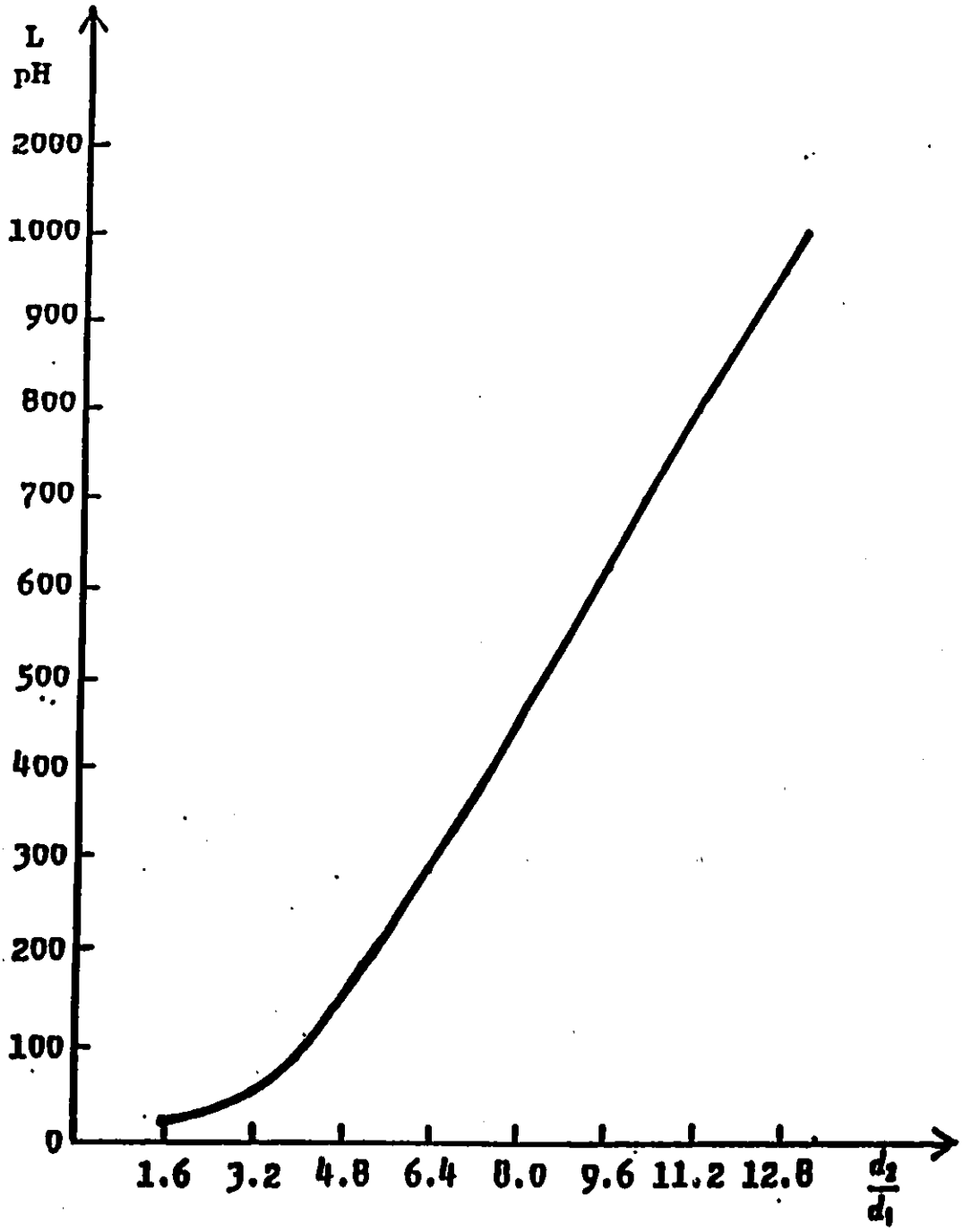

Figure 3.7 The series inductance of an impedance step as a function of the step width ratio in the Ka band.

For the impedance ratio:

$$\frac{Z_2}{Z_1} = \begin{cases} 0.7025 + 0.2975\frac{d_2}{d_1} & 1.0 \leq \frac{d_2}{d_1} \leq 8.8 \\ 1.879 + 0.1639\frac{d_2}{d_1} & 8.8 \leq \frac{d_2}{d_1} \leq 13.6 \end{cases} \tag{3.8}$$

For the inductance:

$$L(in\ pH) = 19.14 - 31.275(\frac{d_2}{d_1}) + 14.56(\frac{d_2}{d_1})^2 - 0.5014(\frac{d_2}{d_1})^3 \tag{3.9}$$

where

$$1.0 \leq \frac{d_2}{d_1} \leq 13.6.$$

The expressions are valid over the following range of parameters:

$$\frac{s}{a} = \frac{1}{28}$$

$$\frac{b}{a} = \frac{1}{2}$$

$$\epsilon_r = 2.2$$

$$1.0 \leq \frac{d_2}{d_1} \leq 13.6$$

$$0.32 \leq \frac{b}{\lambda} \leq 0.47$$

The impedance ratio and the inductance of an impedance step are a function of the dimensions only. They do not vary with frequency since $|\ S_{11}\ |$ is constant over the Ka band as shown in Fig. 3.4. The φ_{11} and φ_{22} do vary with frequency by less than 5 degrees. However, it is obvious that the impedance ratio and the inductance depend more heavily on the ratio $\frac{d_2}{d_1}$ than on frequency.

The abrupt change in the slope of the curve in Fig. 3.6 is due to the fitting of straight lines to the data points. However, the accuracy margin of the impedance ratio cannot be improved by replacing the two straight lines with a smoother curve.

3.4 COMPARISON WITH PUBLISHED RESULTS

In order to compare the empirical expressions with other published methods for the computation of discontinuities, results for impedance steps are presented in Fig. 3.8 which shows the scattering parameters of a step discontinuity obtained by Helard et al. [10] using a combination of spectral domain and mode matching techniques, and considering the first four higher order modes in the two finline sections. These results agree closely with the curves obtained using eqs (3.8) and (3.9) throughout the Ka band, justifying our assumption that the elements of the equivalent circuit for the discontinuity are essentially independent of frequency.

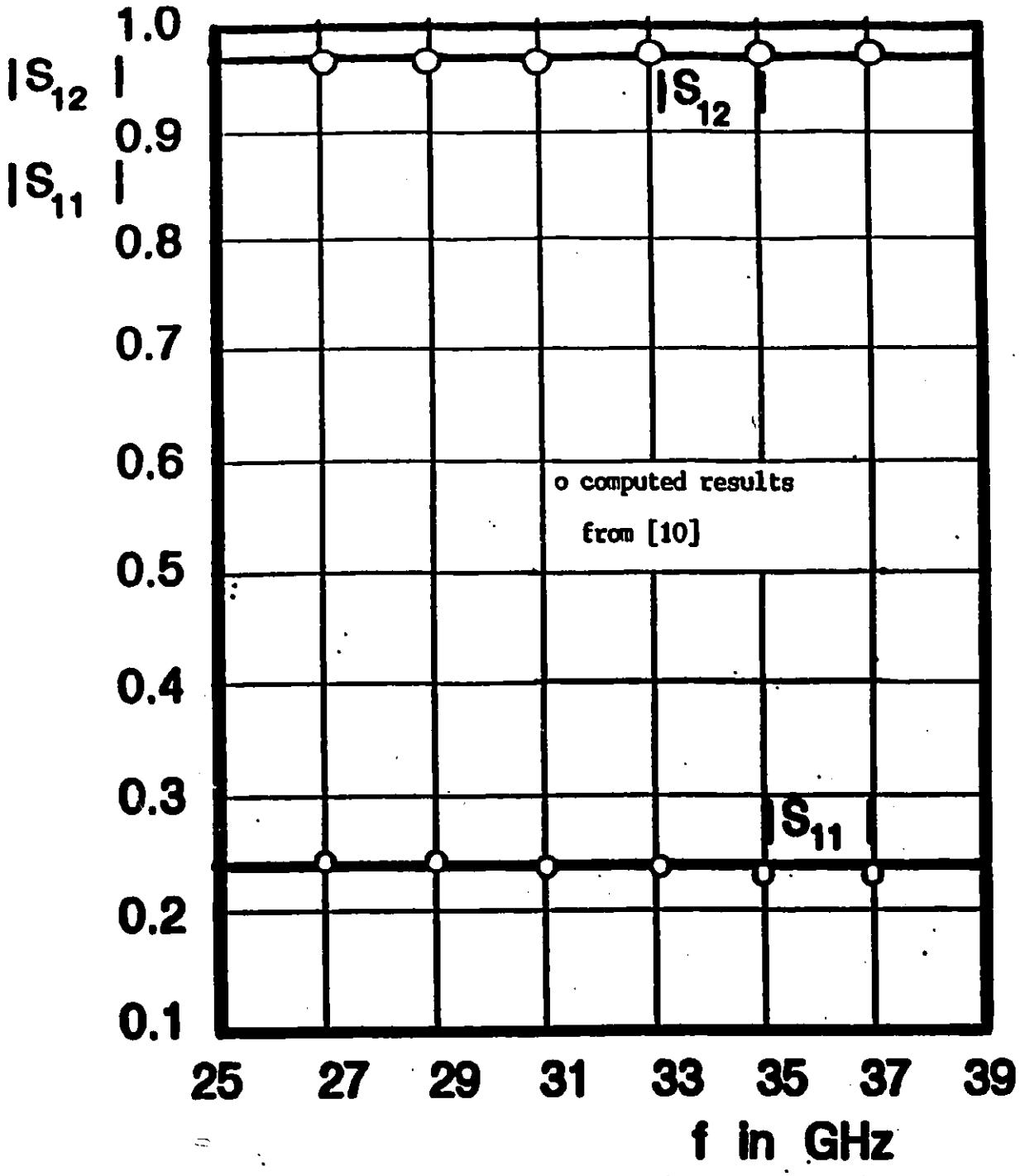

Figure 3.8 Transmission and reflection coefficients of a step discontinuity.

CHAPTER 4

THE DERIVATION AND ACCURACY OF EMPIRICAL FORMULAE OF A SYMMETRICAL INDUCTIVE STRIP

4.1 EQUIVALENT CIRCUIT OF A SYMMETRICAL INDUCTIVE STRIP

As discussed previously, a conducting strip short-circuiting the two fins of a finline, acts as a shunt inductance. Fig. 4.1 shows such a strip and its equivalent circuit. Y_1 and Y_2 represent the characteristic admittances of the two adjacent transmission lines; they are the same in the case of a symmetrical inductive strip. The existence of the shunt susceptance $-jB$ as a parameter of the equivalent circuit accounts for the reactive energy stored by the discontinuity. The electrical excess length $2\Delta\ell$ is partly due to the physical width w of the strip (the reference planes being defined at the edges of the transverse strip), and partly to fringing of the fields in the sharp region.

4.2 THE S-PARAMETERS OF A SYMMETRICAL INDUCTIVE STRIP

As mentioned in Section 3.2, it is advantageous to describe a finline circuit by S-parameters

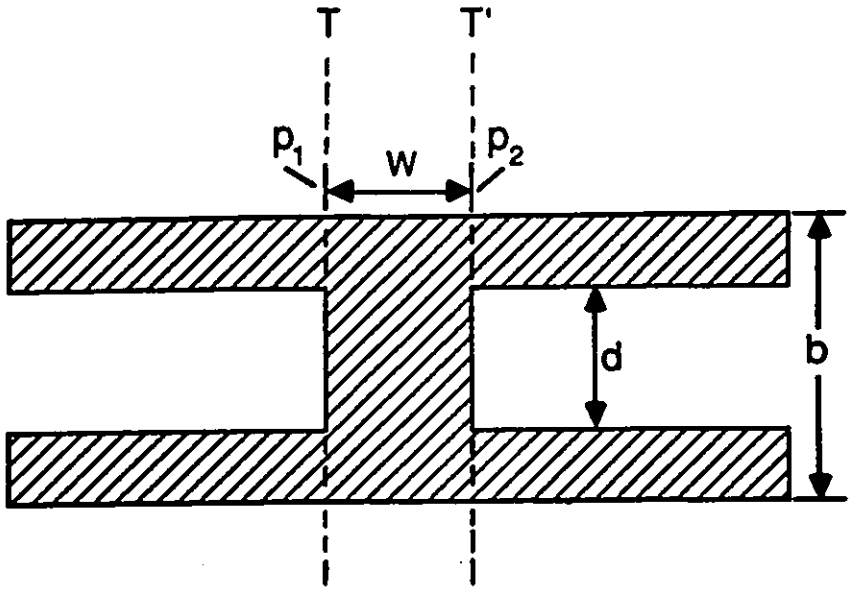

Figure 4.1(a) A symmetrical inductive strip.

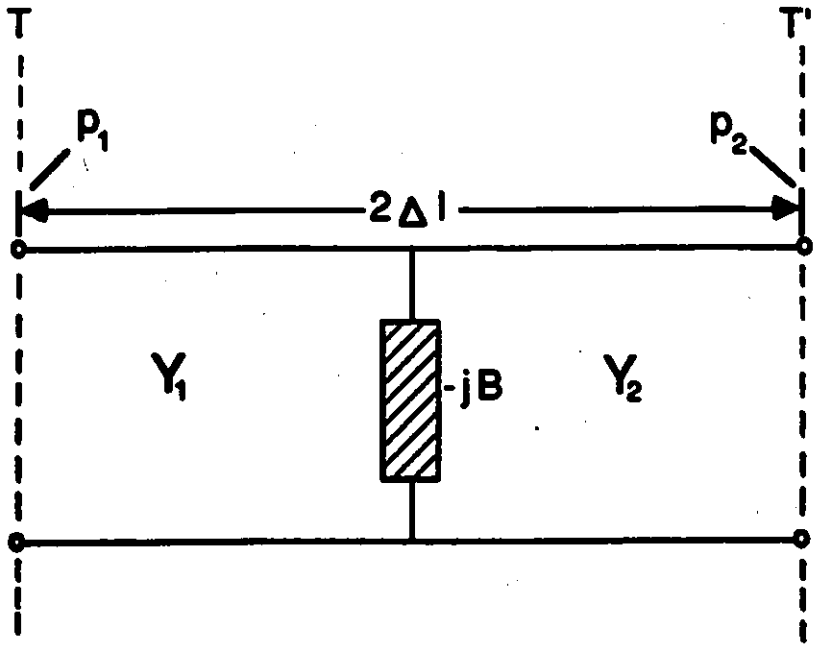

Figure 4.1(b) Equivalent circuit of a symmetrical inductive strip.

Figure 4.1 A symmetrical inductive strip and its equivalent circuit.

because of its ease of measurement at microwave frequencies. As in the case of the step impedance, the scattering matrix coefficients of a symmetrical inductive strip are formulated in terms of the equivalent circuit parameters. Using the symbols of the equivalent circuit parameters in Fig. 4.1, the scattering parameters of the symmetrical inductive strip can be expressed as:

$$S_{11} = \frac{-j\frac{-B}{Y_1}}{(2+j\frac{-B}{Y_1})(cosh(\gamma\Delta\ell)+sinh(\gamma\Delta\ell))^2} \tag{4.1}$$

$$S_{12} = \frac{2}{(2+j\frac{-B}{Y_1})(cosh(\gamma\Delta\ell)+sinh(\gamma\Delta\ell))^2} \tag{4.2}$$

$$S_{21} = S_{12} \tag{4.3}$$

$$S_{22} = S_{11} \tag{4.4}$$

where γ is the propagation constant.

Equation (4.3) expresses the fact that the symmetrical inductive strip is a reciprocal network. Equation (4.4) applies because $Y_1 = Y_2$. The derivation of equations (4.1) and (4.2) can be found in Appendix C.

The equivalent voltages are chosen in such a way that power is given by $\frac{1}{2}\frac{|V_n^+|^2}{Z_0}$ for all modes in the evaluation of the S-parameters in equations (4.1) to (4.4). The reason for doing so is explained in Section 3.2. The empirical formulae for the equivalent circuit parameters are derived in Section 4.3.

4.3 THE DERIVATION OF EMPIRICAL FORMULAE FOR A SYMMETRICAL INDUCTIVE STRIP

Koster and Jansen [11] have evaluated the normalized shunt susceptance $\frac{-B}{Y_1}$ of a sym-

metrical inductive strip at various $\frac{w}{b}$ ratios at 8, 10, and 13 GHz for a strip width of $d = 1.27$ mm. Their computed result is shown in Fig. 4.2. The empirical formula for the normalized shunt susceptance $\frac{-B}{Y_1}$ is derived as follows:

(1) An expression for $\frac{-B}{Y_1}$ in terms of the $\frac{w}{b}$ ratio at frequency $f = 10$ GHz and $\frac{b}{d} = 8$ is obtained using the data in Fig. 4.2. It is found as:

$$(\frac{-B}{Y_1})_{\substack{f=10GHz \\ \frac{b}{d}=8}} = 2.778 + 39.26(\frac{w}{b}) - 33.43(\frac{w}{b})^2 + 111.4(\frac{w}{b})^3 \tag{4.5}$$

(2) The values for $\frac{-B}{Y_1}$ are then sampled at 8, 10, and 13 GHz for each $\frac{w}{b}$ value. The sampled values are contained in Table 4.1. $\frac{-B}{Y_1}$ is then expressed in terms of the normalized frequency $\frac{b}{\lambda}$ for each $\frac{w}{b}$ value. Examples of these expressions are:

at $\frac{w}{b} = 0.1$

$$(\frac{-B}{Y_1})_{\substack{\frac{b}{d}=8 \\ \frac{w}{b}=0.1}} = 21.774 - 64.325(\frac{b}{\lambda}) + 57.582(\frac{b}{\lambda})^2 \tag{4.6}$$

at $\frac{w}{b} = 0.3$

$$(\frac{-B}{Y_1})_{\substack{\frac{b}{d}=8 \\ \frac{w}{b}=0.3}} = 61.948 - 217.82(\frac{b}{\lambda}) + 229.58(\frac{b}{\lambda})^2 \tag{4.7}$$

(3) In order to generate normalized shunt susceptance values at intermediate frequencies, the normalized frequency $\frac{b}{\lambda}$ (corresponding to any intermediate frequency) is substituted into the expressions in Table 4.1. The rms value of $\frac{-B}{Y_1}$ is then calculated. A numerical example for an intermediate frequency at 11 GHz (or $\frac{b}{\lambda} = 0.3726$) is presented in Table 4.2. This procedure is repeated with other $\frac{b}{\lambda}$ values between 0.2710 (corresponding to 8 GHz) and 0.4403 (corresponding to 13 GHz).

(4) The frequency factor is defined as:

$$frequency\ factor = \frac{(\frac{-B}{Y_1})_{\frac{b}{d}=8}^{f}}{(\frac{-B}{Y_1})_{\substack{f=10GHz \\ \frac{b}{d}=8}}} \tag{4.8}$$

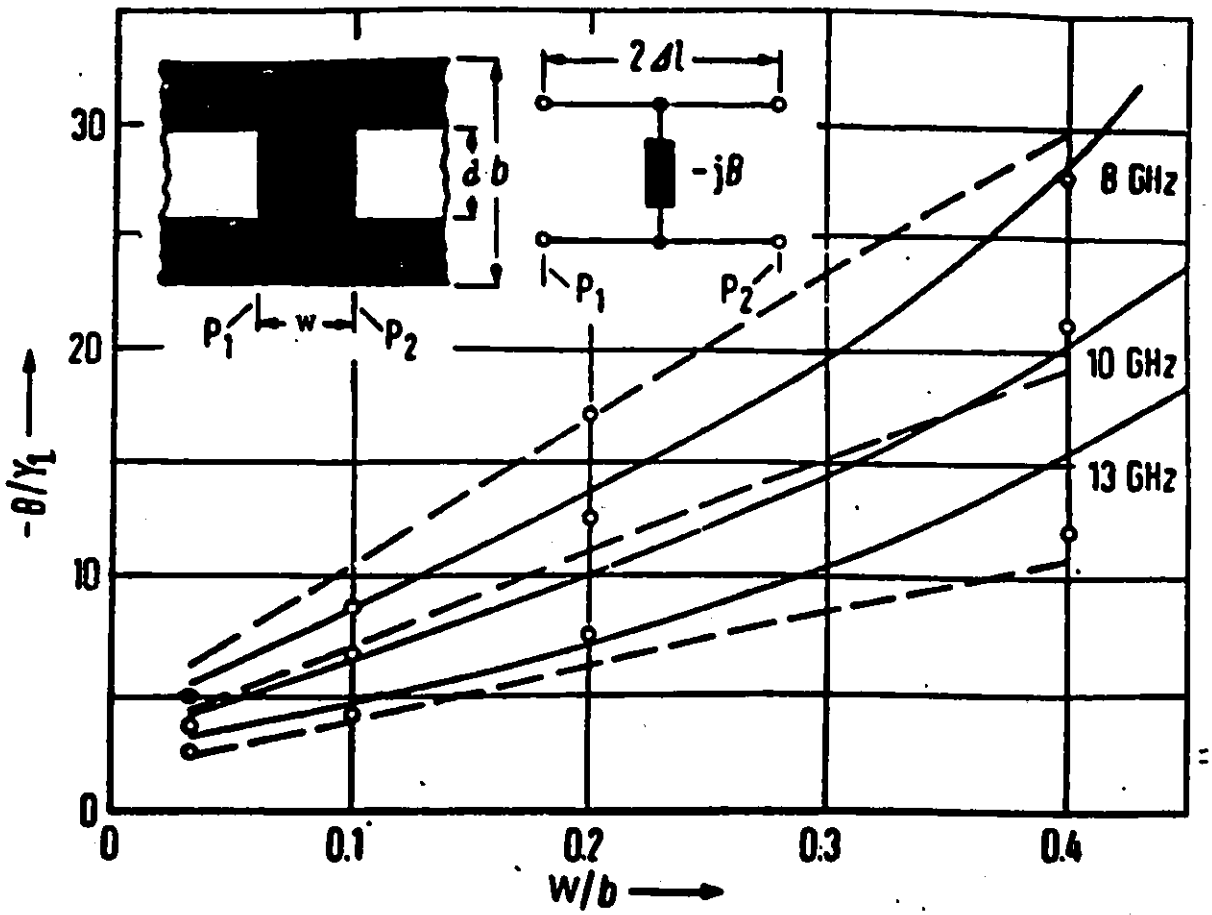

Figure 4.2 The computed result of normalized shunt susceptance as a function of the normalized inductive strip widths $\frac{w}{b}$ in [11].
Other dimensions are: a = 20.32 mm, b = 10.16 mm, h = 0.635 mm, $\varepsilon_r = 2.22$, $\frac{b}{d} = 8$.
0 0 0 measurements in [17].
----- formula developed in [17].
——— rigorous computation in [11].

Table 4.1

Normalized shunt susceptance of a transverse strip derived from sampled values of $\frac{-B}{Y_1}$ at different frequencies and $\frac{w}{b}$ ratios .

$\frac{w}{b}$	$f = 8GHz$ $\frac{b}{\lambda} = 0.2710$	$f = 10GHz$ $\frac{b}{\lambda} = 0.3387$	$f = 13GHz$ $\frac{b}{\lambda} = 0.4403$	FORMULAE
0.05	6.264	4.615	3.626	$\frac{-B}{Y_1} = 20.793 - 77.02\left(\frac{b}{\lambda}\right) + 86.375\left(\frac{b}{\lambda}\right)^2$
0.10	8.571	6.593	4.615	$\frac{-B}{Y_1} = 21.774 - 64.325\left(\frac{b}{\lambda}\right) + 57.582\left(\frac{b}{\lambda}\right)^2$
0.15	11.21	8.242	5.934	$\frac{-B}{Y_1} = 34.543 - 119.91\left(\frac{b}{\lambda}\right) + 124.77\left(\frac{b}{\lambda}\right)^2$
0.20	13.52	10.22	7.253	$\frac{-B}{Y_1} = 37.324 - 119.12\left(\frac{b}{\lambda}\right) + 115.43\left(\frac{b}{\lambda}\right)^2$
0.25	16.48	12.20	8.901	$\frac{-B}{Y_1} = 50.284 - 173.96\left(\frac{b}{\lambda}\right) + 181.63\left(\frac{b}{\lambda}\right)^2$
0.30	19.78	14.51	10.55	$\frac{-B}{Y_1} = 61.948 - 217.82\left(\frac{b}{\lambda}\right) + 229.58\left(\frac{b}{\lambda}\right)^2$
0.35	23.41	17.14	12.86	$\frac{-B}{Y_1} = 75.881 - 274.44\left(\frac{b}{\lambda}\right) + 298.22\left(\frac{b}{\lambda}\right)^2$
0.40	28.35	20.44	15.49	$\frac{-B}{Y_1} = 96.945 - 362.15\left(\frac{b}{\lambda}\right) + 402.35\left(\frac{b}{\lambda}\right)^2$

Assumption : $\frac{b}{d} = 8$

TABLE 4.2

Normalized shunt susceptance values of a transverse strip at various $\frac{w}{b}$ ratios at 11 GHz .

$\frac{w}{b}$	$\frac{-B}{Y_1}$
0.05	4.087
0.10	5.801
0.15	7.186
0.20	8.965
0.25	10.682
0.30	12.661
0.35	15.027
0.40	17.866

RMS value of $\frac{-B}{Y_1}$ is 11.190.

Assumptions : f = 11 GHz $\left(\frac{b}{\lambda}=0.3726\right)$ and $\frac{b}{d}=8$

where

$(\frac{-B}{Y_1})_{\substack{f \\ \frac{b}{d}=8}}$ is the normalized shunt susceptance at frequency f in GHz as the rms values obtained with procedure (3) at $\frac{b}{d} = 8$ and

$(\frac{-B}{Y_1})_{\substack{f=10GHz \\ \frac{b}{d}=8}}$ is the normalized shunt susceptance corresponding to f = 10 GHz obtained with procedure (3), also at $\frac{b}{d} = 8$

Fitting a smooth curve through the various frequency factor values, an expression for the frequency factor in terms of $\frac{b}{\lambda}$ is obtained.

$$frequency\ factor = 4.156 - 14.472(\frac{b}{\lambda}) + 15.218(\frac{b}{\lambda})^2 \tag{4.9}$$

The graph of the frequency factor versus $\frac{b}{\lambda}$ is plotted on Fig. 4.3.

(5) Using the laboratory measurement results [17] shown in Fig. 4.4, an expression for $\frac{-B}{Y_1}$ in terms of the $\frac{w}{b}$ ratio at f = 8 GHz and $\frac{b}{d} = 8$ is obtained.

(6) At each $\frac{w}{b}$ value, $\frac{-B}{Y_1}$ is read at the three different $\frac{b}{d}$ ratios in Fig. 4.4. Quadratic expressions of $\frac{-B}{Y_1}$ in terms of $\frac{b}{d}$ are then obtained at each $\frac{w}{b}$ ratio. These expressions are similar to equations (4.6) and (4.7) except that $\frac{b}{\lambda}$ is replaced by $\frac{b}{d}$. They are presented in Table 4.3.

(7) The following steps are taken to generate $\frac{-B}{Y_1}$ at intermediate $\frac{b}{d}$ ratios: $\frac{b}{d}$ values between 4 and 16 are substituted into the expressions in Table 4.3; the rms value of $\frac{-B}{Y_1}$ is then calculated. A numerical example with $\frac{b}{d} = 10$ is shown in Table 4.4. This procedure is repeated with other $\frac{b}{d}$ ratios.

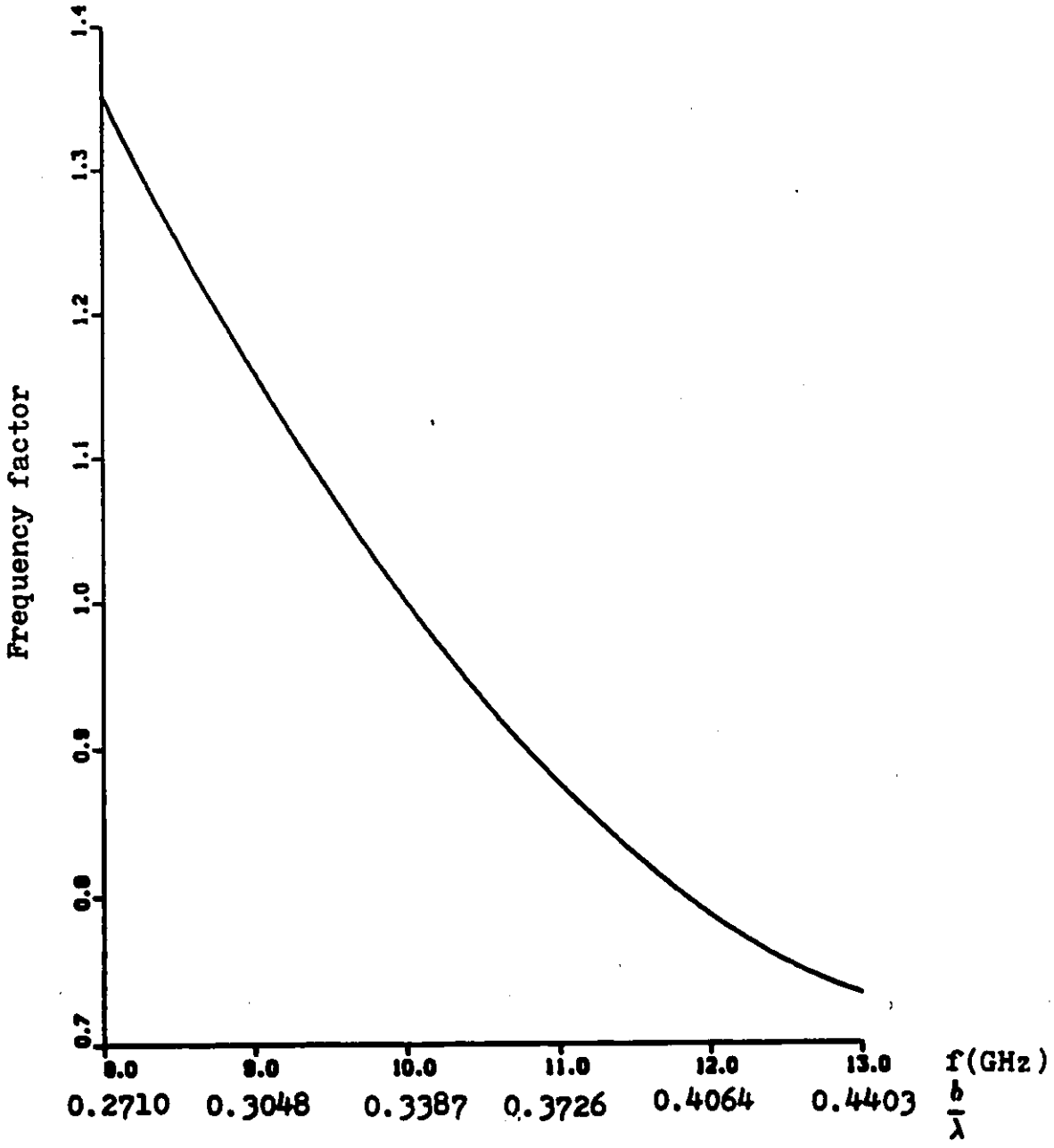

Figure 4.3 A plot of frequency factor versus frequency or $\frac{b}{\lambda}$.

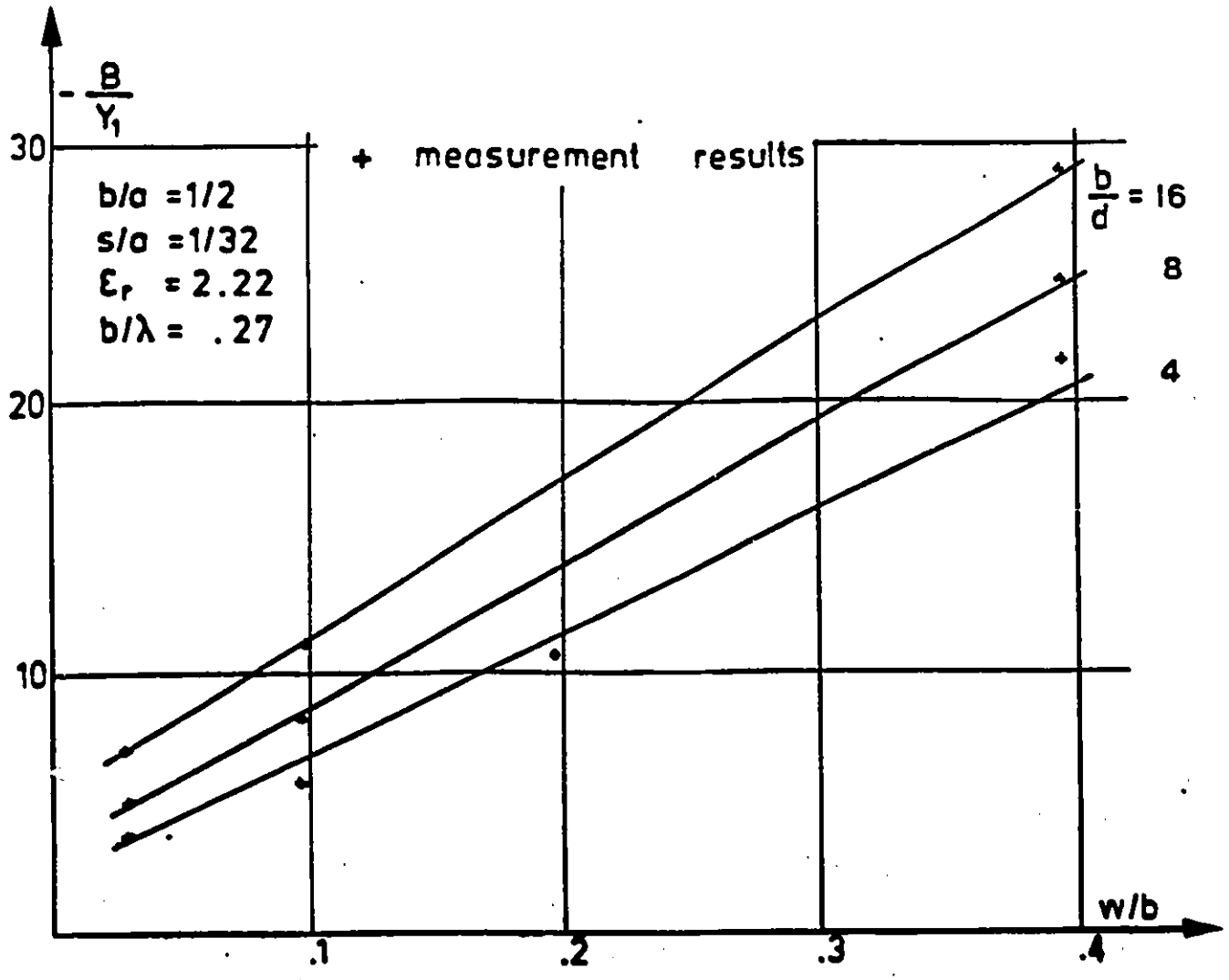

Figure 4.4 Laboratory measurement results of $\frac{-B}{Y_1}$ with various $\frac{w}{b}$ ratio.

Table 4.3

Normalized shunt susceptance of a transverse strip derived from sampled values at different $\frac{b}{d}$ and $\frac{w}{b}$ ratios .

$\frac{w}{b}$	$\frac{b}{d}=4$	$\frac{b}{d}=8$	$\frac{b}{d}=16$	FORMULAE
0.10	7.005	8.664	11.24	$\frac{-B}{Y_1}=5.099+0.5075\left(\frac{b}{d}\right)-0.007729\left(\frac{b}{d}\right)^2$
0.20	11.06	13.64	17.14	$\frac{-B}{Y_1}=7.927+0.8525\left(\frac{b}{d}\right)-0.01729\left(\frac{b}{d}\right)^2$
0.30	15.85	19.08	22.86	$\frac{-B}{Y_1}=11.727+1.1425\left(\frac{b}{d}\right)-0.02792\left(\frac{b}{d}\right)^2$
0.40	20.46	24.42	28.76	$\frac{-B}{Y_1}=15.307-1.4375\left(\frac{b}{d}\right)-0.03729\left(\frac{b}{d}\right)^2$

TABLE 4.4

Normalized shunt susceptance values of a transverse strip at various $\frac{w}{b}$ ratios .

$\frac{w}{b}$	$\frac{-B}{Y_1}$
0.1	9.401
0.2	14.72
0.3	20.36
0.4	25.95

RMS value of $\frac{-B}{Y_1}$ is 18.66 .

Assumptions : $\frac{b}{d} = 10$ and $\frac{b}{\lambda} = 0.27$

(8) Defining the dimension factor as follows:

$$dimension\ factor = \frac{(\frac{-B}{Y_1})_{f=8GHz,\ \frac{b}{d}}}{(\frac{-B}{Y_1})_{f=8GHz,\ \frac{b}{d}=8}} \tag{4.10}$$

where

$(\frac{-B}{Y_1})_{f=8GHz,\ \frac{b}{d}}$ is the normalized shunt susceptance at any $\frac{b}{d}$ ratio obtained as the rms values with procedure (7) at f = 8 GHz.

$(\frac{-B}{Y_1})_{f=8GHz,\ \frac{b}{d}=8}$ is the normalized shunt susceptance at $\frac{b}{d} = 8$ obtained with procedure (7), also at f = 8 GHz.

Fitting a smooth curve through all the dimension factor values, an expression for the dimension factor in terms of $\frac{b}{d}$ is obtained.

$$dimension\ factor = 0.6046 + 0.05926(\frac{b}{d}) - 0.001224(\frac{b}{d})^2 \tag{4.11}$$

Fig. 4.5 shows the graph of the dimension factor versus $\frac{b}{d}$ ratio.

The procedures in deriving the empirical formulae of $\frac{-B}{Y_1}$ can be summarized in a few sentences. First of all, a cubical expression of $\frac{-B}{Y_1}$ in terms of $\frac{w}{b}$ is obtained at $f = 10$ GHz and at $\frac{b}{d} = 8$. Then the frequency factor and the dimension factor are obtained in terms of $\frac{b}{\lambda}$ and $\frac{b}{d}$ respectively. After deriving these three quantities, the closed-form expression of the normalized shunt susceptance $\frac{-B}{Y_1}$ is found as [25] :

$$\frac{-B}{Y_1} = (\frac{-B}{Y_1})_{f=10GHz,\ \frac{b}{d}=8} \times [\text{frequency factor}] \times [\text{dimension factor}]$$

$$\frac{-B}{Y_1} = [2.778 + 39.26(\frac{w}{b}) - 33.43(\frac{w}{b})^2 + 111.4(\frac{w}{b})^3] \times [4.156 - 14.472(\frac{b}{\lambda}) + 15.218(\frac{b}{\lambda})^2]$$

$$\times [0.6046 + 0.05926(\frac{b}{d}) - 0.001224(\frac{b}{d})^2] \tag{4.12}$$

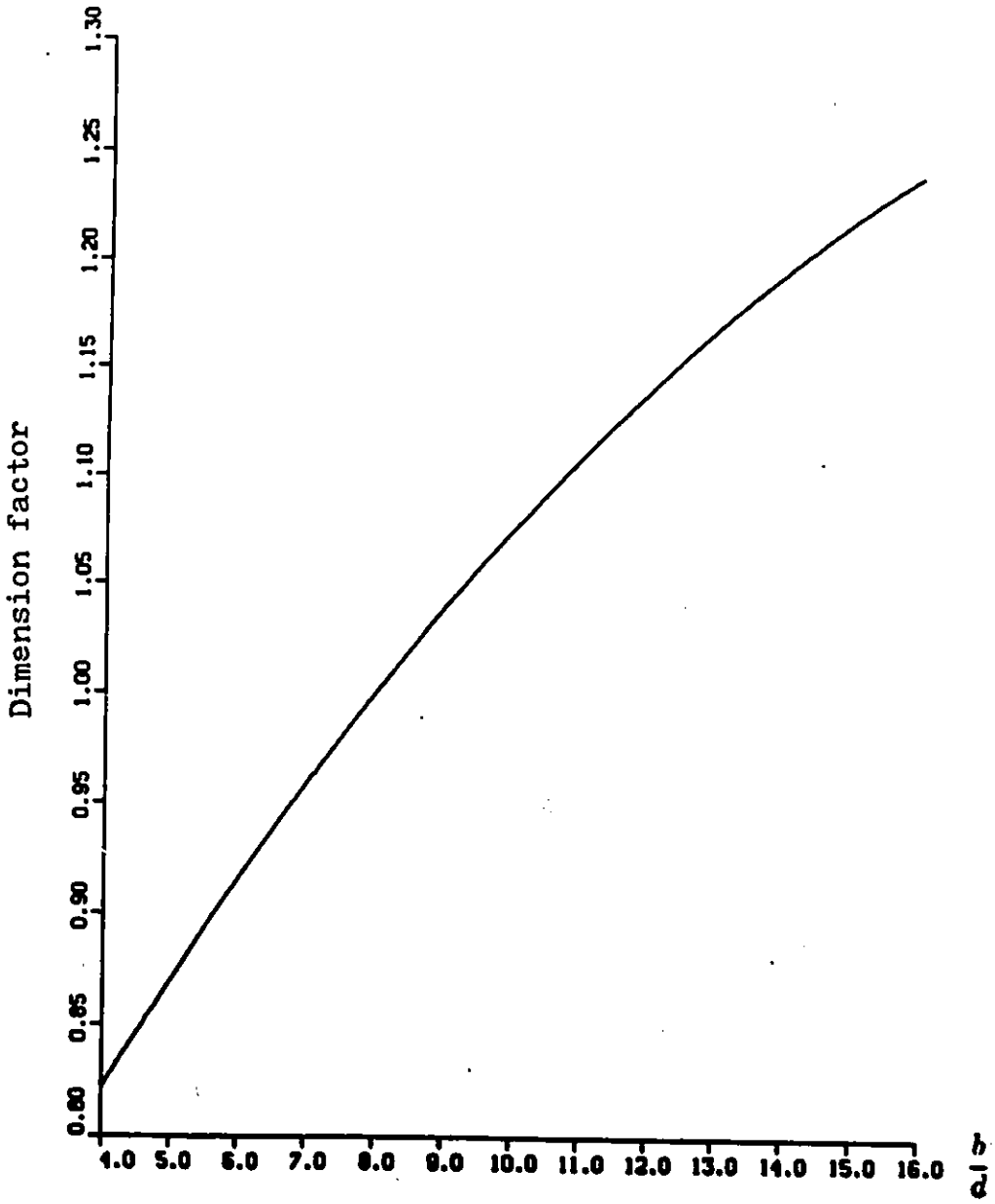

Figure 4.5 The dimension factor is plotted as a function of $\frac{b}{d}$.

The derivation of the normalized excess electrical length requires a different approach and is comparatively easier. Fig. 4.6 and Fig. 4.7 show the measurement results [17] for the normalized excess electrical length $\frac{\Delta\ell}{b}$ at various $\frac{w}{b}$ ratios, $\frac{d}{b} = \frac{1}{4}, \frac{1}{8}, \frac{1}{16}$, and $\frac{b}{\lambda} = 0.27, 0.473$.

The empirical formula of the normalized excess electrical length $\frac{\Delta\ell}{b}$ is derived as follows:

(a) $\frac{\Delta\ell}{b}$ is expressed as a function of $\frac{w}{b}$ in the form of

$$\frac{\Delta\ell}{b} = A + B(\frac{w}{b}) + C(\frac{w}{b})^2 + D(\frac{w}{b})^3 + E(\frac{w}{b})^4 \qquad (4.13)$$

Thus, six equations are found for the curves shown in Fig. 4.6 and Fig. 4.7 to determine the coefficients A to E.

(b) Defining a coefficient ratio as follows:

$$\mathcal{A}_A^1 = \frac{A^1}{A_{\frac{1}{8}}^1} \qquad (4.14)$$

where

A^1 = coefficient A at $\frac{b}{\lambda} = 0.27$, $\frac{1}{16} \leq \frac{d}{b} \leq \frac{1}{4}$

$A_{\frac{1}{8}}^1$ = coefficient A at $\frac{b}{\lambda} = 0.27$, $\frac{d}{b} = \frac{1}{8}$.

The superscript '1' stands for $\frac{b}{\lambda} = 0.27$ while '11' stands for $\frac{b}{\lambda} = 0.473$.

A quadratic expression for $\mathcal{A}_A^1$ in terms of $\frac{d}{b}$ is found by substituting the values of A^1 at $\frac{d}{b} = \frac{1}{4}, \frac{1}{8}, \frac{1}{16}$ into equation (4.14). It is found to be:

$$\mathcal{A}_A^1 = -0.09806 + 12.464(\frac{d}{b}) - 29.432(\frac{d}{b})^2 \quad 0.05 \leq \frac{w}{b} \leq 0.1 \qquad (4.15)$$

Similarly, another coefficient ratio at $\frac{b}{\lambda} = 0.473$ is defined as

$$\mathcal{A}_A^{11} = \frac{A^{11}}{A_{\frac{1}{8}}^1}$$

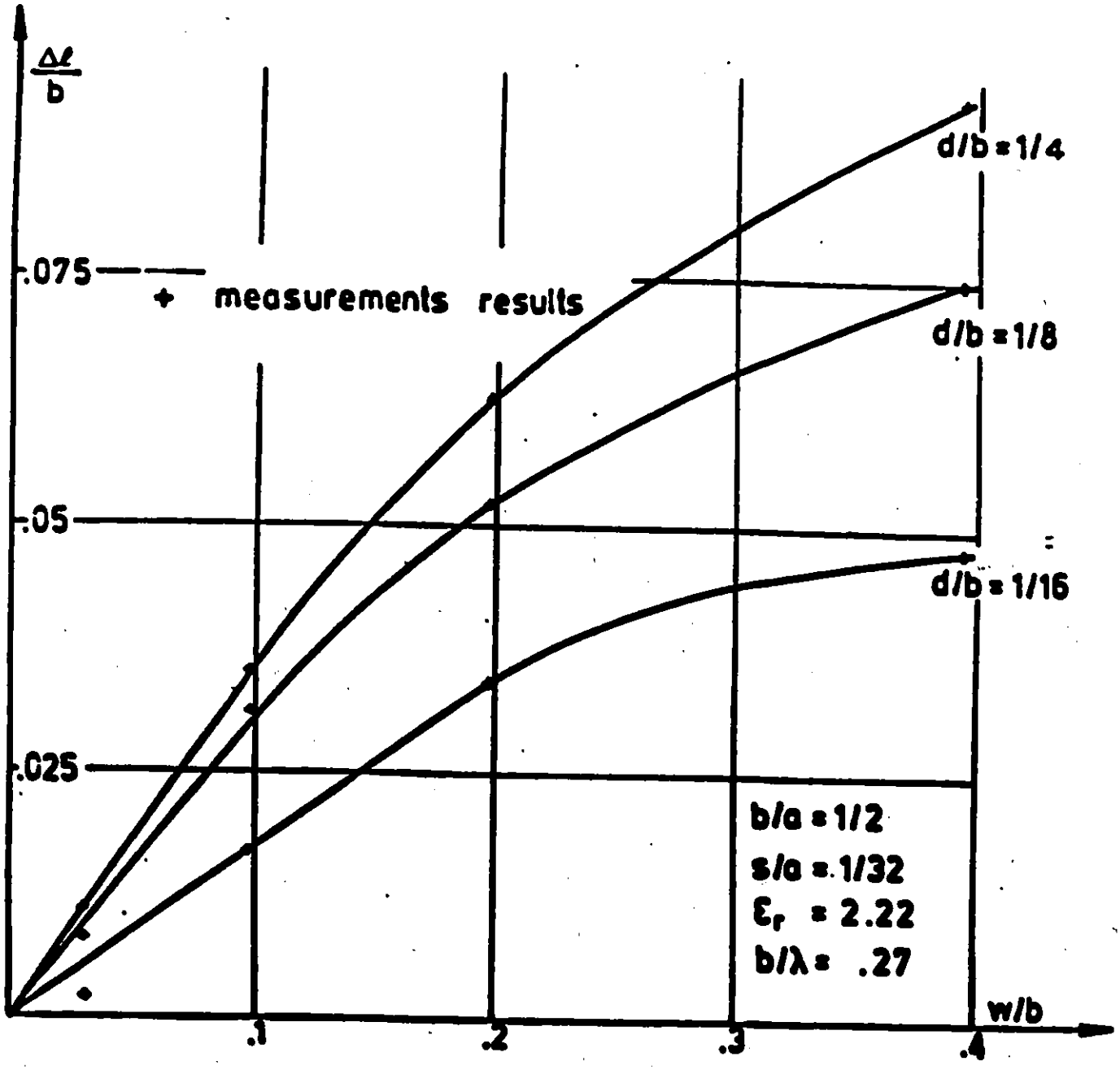

Figure 4.6 Laboratory measurement results of the normalized electrical length $\frac{\Delta \ell}{b}$ of a symmetrical inductive strip. Note that the slopes of the curves change drastically at $\frac{w}{b} = 0.1$ and $\frac{b}{\lambda} = .27$.

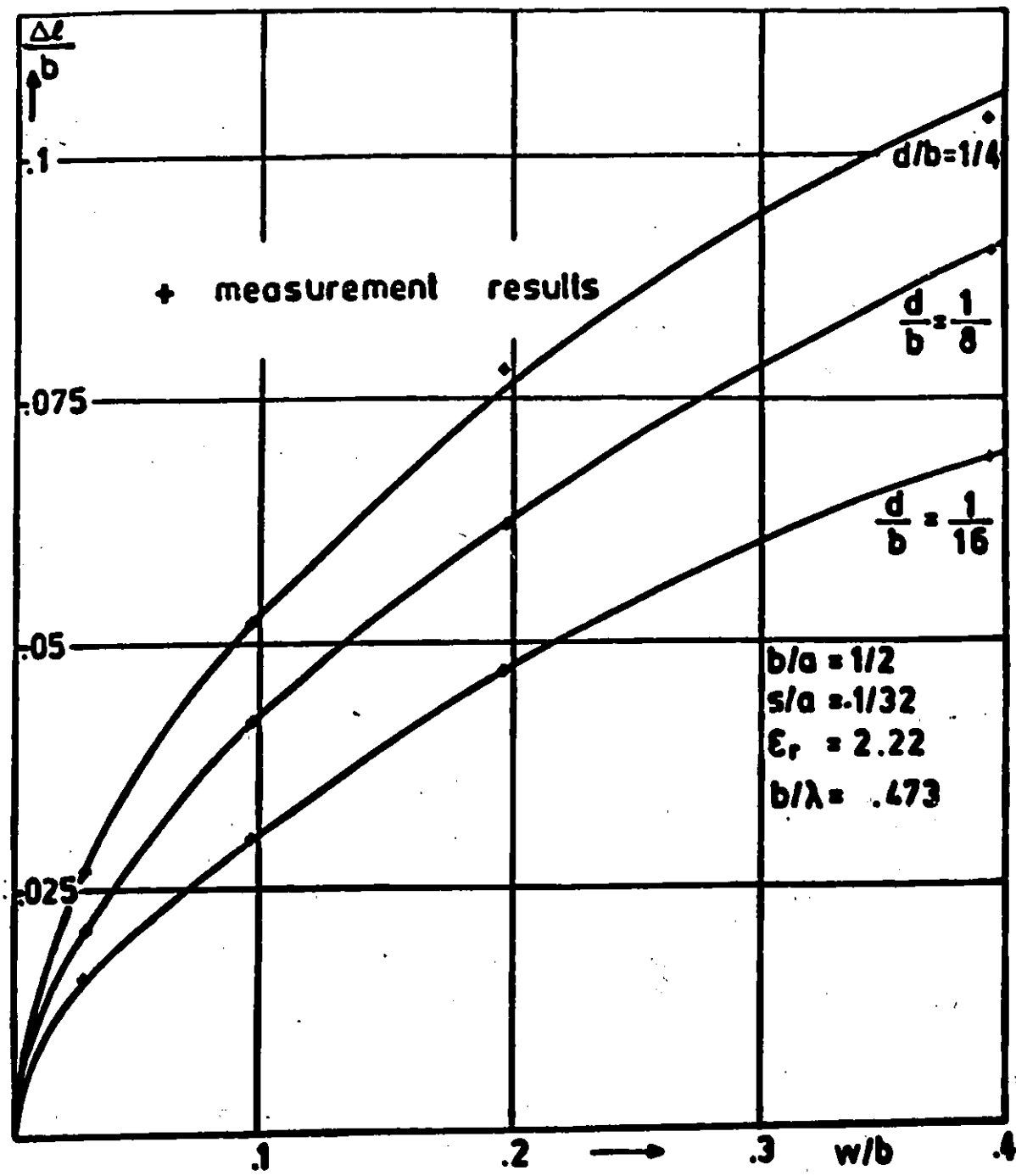

Figure 4.7 Laboratory measurement results of the normalized electrical length $\frac{\Delta\ell}{b}$ of a symmetrical inductive strip. Note that the slopes of the curves change drastically at $\frac{w}{b} = 0.1$ and $\frac{b}{\lambda} = .473$.

where $\mathcal{A}^{11}$ = coefficient A at $\frac{b}{\lambda} = 0.473$, $\frac{1}{16} \leq \frac{d}{b} \leq \frac{1}{4}$.

$\mathcal{A}_A^{11}$ can be expressed as a quadratic equation in terms of $\frac{d}{b}$ similar to equation (4.15).

(c) Since the measurements of $\frac{\Delta f}{b}$ were available at $\frac{b}{\lambda} = 0.27$ and $\frac{b}{\lambda} = 0.473$ only, a linear dependence of $\frac{\Delta f}{b}$ on frequency is assumed. To account for the frequency dependence of $\frac{\Delta f}{b}$, a third quantity is defined as:

$$\mathcal{Y}_A = \frac{A}{\mathcal{A}_{\frac{b}{\lambda}}^1} \tag{4.16}$$

where A = coefficient A at $\frac{1}{16} \leq \frac{d}{b} \leq \frac{1}{4}$ and $0.27 \leq \frac{b}{\lambda} \leq 0.473$.

$\mathcal{Y}_A$ is the expression of the straight line relating $\mathcal{A}_A$ and $\frac{b}{\lambda}$. In this case, we can express $\mathcal{Y}_A$ in the following form:

$$\mathcal{Y}_A = \frac{\mathcal{A}_A^{11} - \mathcal{A}_A^1}{0.473 - 0.27}\left(\frac{b}{\lambda} - 0.473\right) + \mathcal{A}_A^{11} \tag{4.17}$$

Thus, at $\frac{b}{\lambda} = 0.473$, $\mathcal{Y}_A = \mathcal{A}_A^{11}$ and equation (4.16) follows. Similarly, at $\frac{b}{\lambda} = 0.27$, $\mathcal{Y}_A = \mathcal{A}_A^1$ and equation (4.16) follows.

Procedures (b) and (c) are repeated for all other coefficients in the equation (4.13).

The empirical formula of $\frac{\Delta f}{b}$ thus derived is found as [25]:

$$\frac{\Delta f}{b} = \mathcal{Y}_A(0.2995)\left(\frac{w}{b}\right) + \mathcal{Y}_B(-3.562)\left(\frac{w}{b}\right)^2 \qquad 0.05 \leq \frac{w}{b} \leq 0.1 \tag{4.18}$$

where

$$\mathcal{Y}_i = \frac{\mathcal{A}_i^{11} - \mathcal{A}_i^1}{0.203}\left(\frac{b}{\lambda} - 0.473\right) + \mathcal{A}_i^{11} \qquad i = A, B \tag{4.19}$$

$$\mathcal{A}_A^{11} = 1.185 + 13.559\left(\frac{d}{b}\right) - 17.958\left(\frac{d}{b}\right)^2 \tag{4.20}$$

$$\mathcal{A}_A^1 = -0.09806 + 12.464\left(\frac{d}{b}\right) - 29.432\left(\frac{d}{b}\right)^2 \tag{4.21}$$

$$\mathcal{X}_B^{11} = 0.62135 + 2.8438(\frac{d}{b}) + 1.4831(\frac{d}{b})^2 \tag{4.22}$$

$$\mathcal{X}_B^{1} = 0 \tag{4.23}$$

$\mathcal{X}_B^1$ is zero indicates that for $\frac{b}{\lambda}$ is 0.27 and for the range $0.05 \leq \frac{w}{b} \leq 0.1$, the dependence of $\frac{\Delta\ell}{b}$ on $\frac{w}{b}$ is linear. This is shown in Fig. 4.6. Since $B_{\frac{1}{8}}^1$ is zero, it is replaced by $B_{\frac{1}{8}}^{11}$. In this case, the constants in equation (4.18), 0.2995 and -3.562, are $A_{\frac{1}{8}}^1$ and $B_{\frac{1}{8}}^{11}$ respectively. Note that for $\frac{b}{\lambda}$ is 0.27, $\frac{\Delta\ell}{b}$ is a linear equation in terms of $\frac{w}{b}$.

$$\frac{\Delta\ell}{b} = \mathcal{Y}_A(-0.0004874) + \mathcal{Y}_B(0.3179)(\frac{w}{b}) + \mathcal{Y}_C(0.0925)(\frac{w}{b})^2 + \mathcal{Y}_D(-2.563)(\frac{w}{b})^3 + \mathcal{Y}_E(3.885)(\frac{w}{b})^4 \qquad 0.1 < \frac{w}{b} \leq 0.4 \tag{4.24}$$

where

$$\mathcal{Y}_i = \frac{\mathcal{X}_i^{11} - \mathcal{X}_i^1}{0.203}(\frac{b}{\lambda} - 0.473) + \mathcal{X}_i^{11} \qquad i = A, B, ..., E \tag{4.25}$$

$$\mathcal{X}_A^{11} = -55.557 + 716.52(\frac{d}{b}) - 2505(\frac{d}{b})^2 \tag{4.26}$$

$$\mathcal{X}_A^{1} = -3.70847 + 58.853(\frac{d}{b}) - 169.48(\frac{d}{b})^2 \tag{4.27}$$

$$\mathcal{X}_B^{11} = -1.675 + 45.422(\frac{d}{b}) - 131.98(\frac{d}{b})^2 \tag{4.28}$$

$$\mathcal{X}_B^{1} = -0.4982 + 17.445(\frac{d}{b}) - 43.674(\frac{d}{b})^2 \tag{4.29}$$

$$\mathcal{X}_C^{11} = 58.531 - 1141.5(\frac{d}{b}) + 3447.4(\frac{d}{b})^2 \tag{4.30}$$

$$\mathcal{X}_C^{1} = 15.855 - 183.46(\frac{d}{b}) + 516.99(\frac{d}{b})^2 \tag{4.31}$$

$$\mathcal{X}_D^{11} = 6.9035 - 127.76(\frac{d}{b}) + 389.87(\frac{d}{b})^2 \tag{4.32}$$

$$\mathcal{X}_D^1 = 1.1443 - 2.4656(\frac{d}{b}) + 10.487(\frac{d}{b})^2 \tag{4.33}$$

$$\mathcal{X}_E^{11} = 4.9952 - 90.588(\frac{d}{b}) + 277.26(\frac{d}{b})^2 \tag{4.34}$$

$$\mathcal{X}_E^1 = 0.19323 + 9.1992(\frac{d}{b}) - 21.961(\frac{d}{b})^2 \tag{4.35}$$

The constants in equation (4.24) are the coefficients $A_{\frac{1}{s}}^1$ to $E_{\frac{1}{s}}^1$. Since the slopes of the curves shown in Fig. 4.6 and Fig. 4.7 change drastically around $\frac{w}{b} = 0.1$, two sets of expressions for $\frac{\Delta\ell}{b}$ are developed to represent the curves.

The expressions for normalized shunt susceptance and normalized excess electrical length are valid for the following characteristics and ranges:

$$\frac{b}{a} = \frac{1}{2}$$

$$\frac{s}{a} = \frac{1}{32}$$

$$\varepsilon_r = 2.22$$

$$\frac{1}{16} \leq \frac{d}{b} \leq \frac{1}{4}$$

$$0.05 \leq \frac{w}{b} \leq 0.4$$

$$0.27 \leq \frac{b}{\lambda} \leq 0.44$$

The S-parameters in equations (4.1) to (4.4) can be solved by substituting $\frac{-B}{Y_1}$ in equation (4.12), the propagation constant γ obtained in [9], and the $\frac{\Delta\ell}{b}$ in equations (4.18) to (4.23) or equations (4.24) to (4.35), whichever set of equations is appropriate for the $\frac{w}{b}$ range. $\frac{\Delta\ell}{b}$ is denormalized by multiplying the equations (4.18) or (4.24) by b before the substitution takes place.

4.4 COMPARISION WITH PUBLISHED RESULTS

Besides Koster and Jansen's [11] data and the measurements [17] mentioned in Section 4.3, there are no published data on symmetrical inductive strips in the range and characteristics specified in section 4.3 in the literature up to the time the author did her research, except those by Saad and Schuenemann [13] in the form of transmission and reflection coefficients of a bandpass filter. Fig. 4.8 shows a bandpass filter consisting of two symmetrical inductive strip sections and a transmission line section as indicated. In effect, Fig. 4.8 shows three cascaded two-port networks with the S-parameters in each section known. The S-parameters of a transmission line are found as follows:

$$S_{11} = 0 \tag{4.36}$$

$$S_{12} = e^{-j\gamma\ell} \tag{4.37}$$

$$S_{21} = e^{-j\gamma\ell} \tag{4.38}$$

$$S_{22} = 0 \tag{4.39}$$

The S-parameters of each section of the bandpass filter are obtained using equations (4.1) to (4.4) and equations (4.36) to (4.39).

The ABCD parameters for a two-port network are defined as:

$$\begin{bmatrix} V_1 \\ I_1 \end{bmatrix} = \begin{bmatrix} A & B \\ C & D \end{bmatrix} \begin{bmatrix} V_2 \\ I_2 \end{bmatrix}$$

where

I_1 = current flowing into port 1

I_2 = current flowing out of port 2

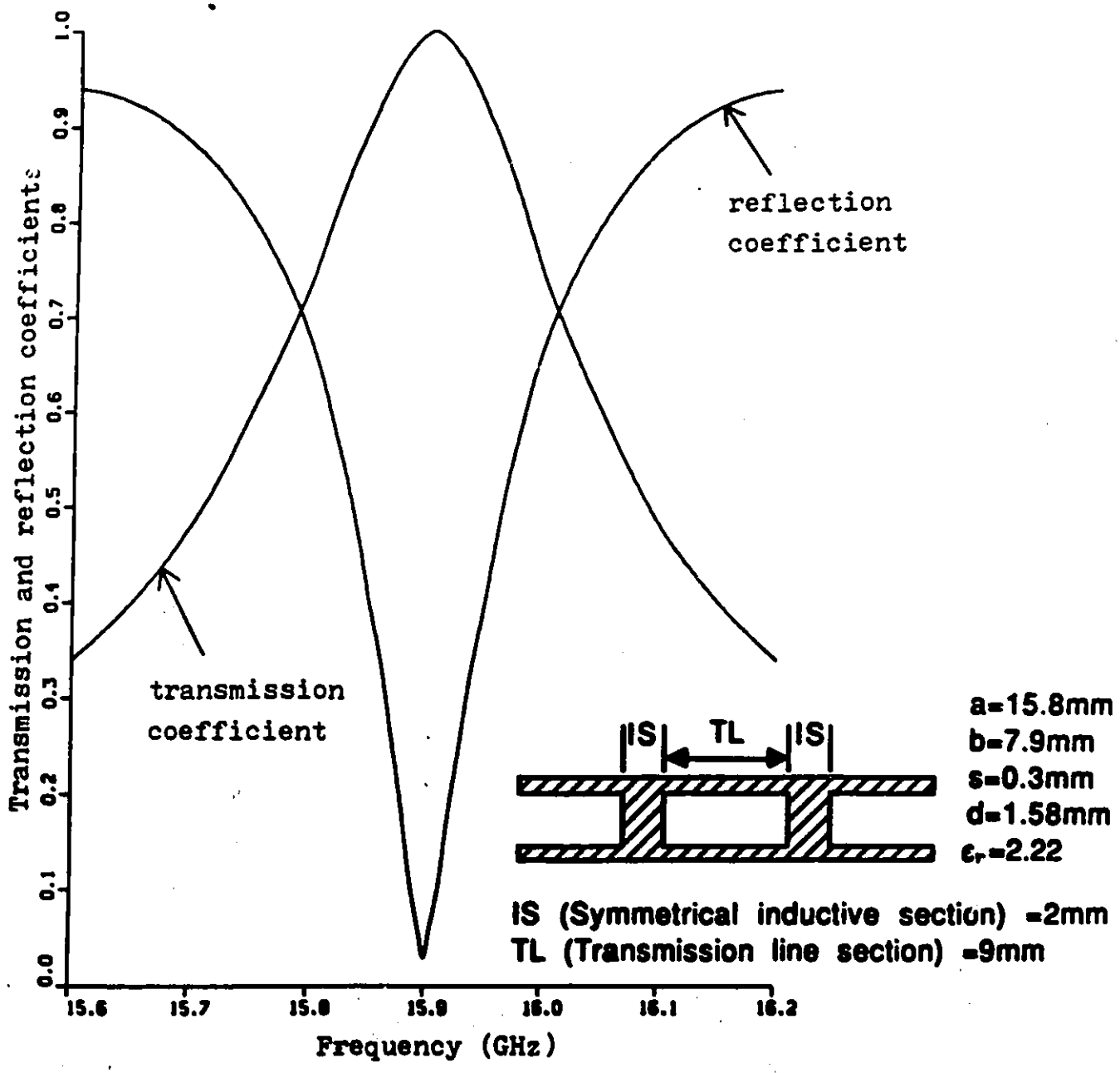

Figure 4.8 The transmission and reflection coefficients of a bandpass filter obtained with the equations derived in Section 4.3.

and V_1 and V_2 are the voltages at port 1 and port 2 respectively.

Since the ABCD matrix of the bandpass filter can be obtained by multiplying the individual ABCD matrices of each section, the S-parameters are transformed into the corresponding ABCD parameters. The overall ABCD matrix is then transformed back into the scattering matrix of the bandpass filter. A computer program has been written to facilitate this transformation. The program will be a handy tool especially when the structures studied become more complicated. A program listing is contained in the Appendix B.

The transmission and reflection coefficients thus obtained are plotted in Fig. 4.8 to compare with the result published in [13] which is shown on Fig. 4.9. However, the response of the bandpass filter has a frequency shift of about 5% comparing to that in [13]. It should be noted that the method of analysis proposed by Saad and Schmenemann is only approximate, and not too much concern should be given to the discrepancies noted above.

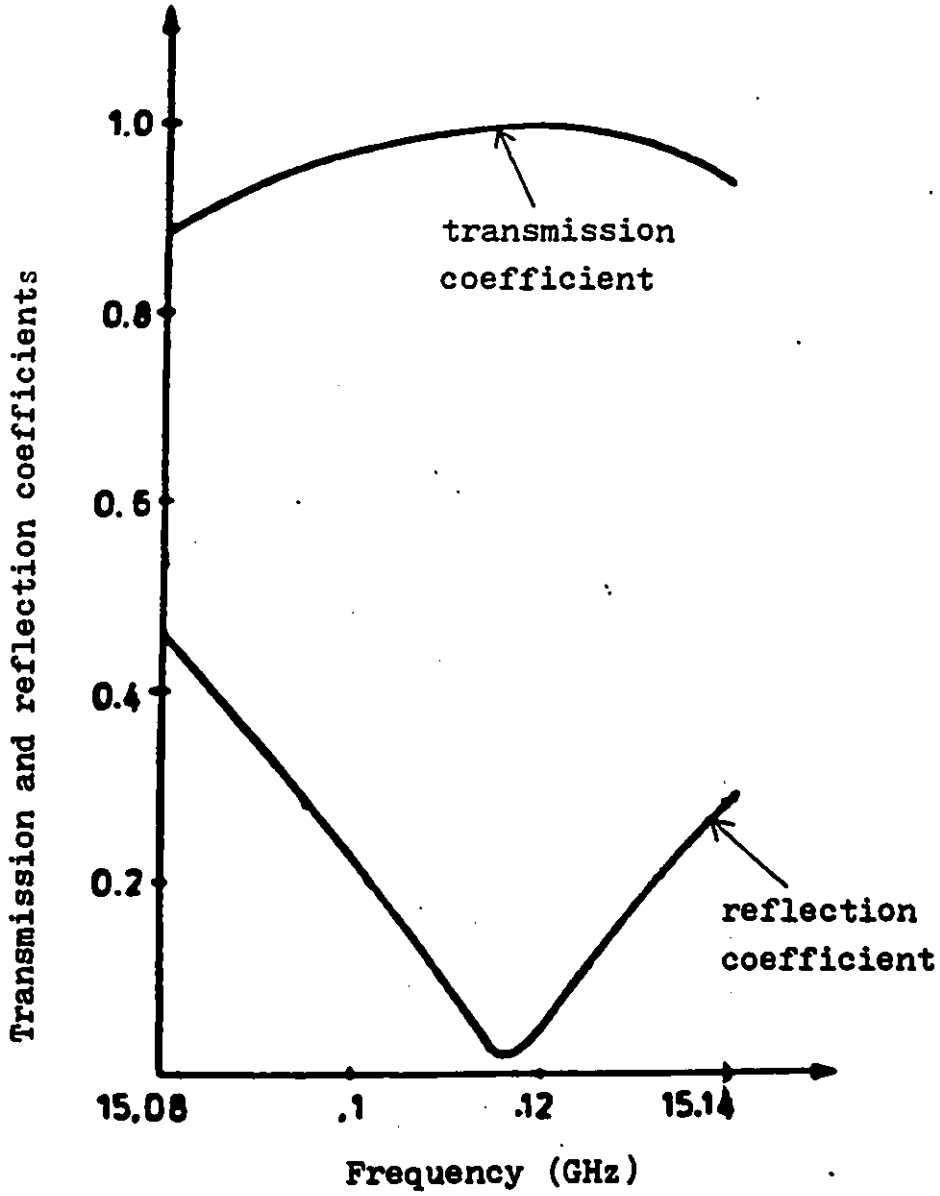

Figure 4.9 The transmission and reflection coefficients of a bandpass filter published in [13] . The dimensions of the bandpass filter are those shown in Figure 4.8.

CHAPTER 5

FUTURE RESEARCH AND CONCLUSION

5.1 FUTURE RESEARCH

Helard et. al. [22], and Webb and Mittra [24] have published papers on step discontinuities. However, the equivalent circuit used by Helard et. al. in [22] to model the step discontinuity is different from the one shown in Fig. 3.1(a) even though the operating frequency range is approximately the same. Webb and Mittra have used another numerical approach in [24] to compute the S-parameters of a step discontinuity operating in the Ka band (i.e. 28 GHz to 40 GHz). So the normalized frequency range is, in effect, the one specified in Section 3.3.

The closed-form expressions for the step impedance and the symmetrical inductive strip in Section 3.3 and Section 4.3, respectively, are valid over a limited range of dimensions and characteristics. Should more published data on these two discontinuities for different dimensions and characteristics become available, closed-form expressions for these two discontinuities could be derived to design most finline circuits consisting of these two discontinuities.

Two papers on symmetrical inductive strips, [27] and [28], have been published after the author had finished her research. Thus, it is beyond the scope of this thesis to discuss them.

Future research could be done to verify the accuracy of the closed-form expressions of the symmetrical inductive strip in this thesis by comparing them with references [27] and [28].

For finline circuits, very tight manufacturing tolerances are desirable to achieve good performance. So, it is worthwhile to study the sensitivity to tolerances of finline structures operating at very high frequency, for example, at 100 GHz.

For more realistic and accurate design, loss should be included in the numerical model. In addition, considerable effort is required to minimize measurement errors in the validation of theoretical models.

Another area of interest is to include the effect of the mounting groove in the discontinuity models.

5.2 CONCLUSION

Empirical formulae for impedance steps and transverse strips in finline have been derived from published experimental and theoretical data. The formulae for the equivalent circuit parameters of the step impedance derived in this thesis are very simple. Yet, the reflection and transmission coefficients of a step impedance computed by the empirical formulea are very close to the data published. Moreover, Pramanick and Bhartia have claimed that the accuracy of the closed-form expressions for a homogeneous unilateral finline in their publication [9] is about $\pm 0.6\%$. Thus, very satisfactory results are obtained by using the empirical formulae of the step impedance in combination with their expressions.

The procedures employed in deriving the closed-form expressions of the symmetrical induc-

tive strip are more complicated than those for a step impedance, and the resulting expressions are also more complex than those for the latter.

The main advantage of these expressions and models is that they can easily be incorporated in a CAD program, and to allow the designer to employ dimensions other than those chosen by the few authors that have published results so far.

APPENDIX A

THE S-PARAMETERS OF A STEP FROM 30 TO 40 GHZ

A = 7.112000 MM
B = 3.556000 MM
S = 0.254000 MM
ER = 2.220000

NE	ELN	IP	JP	KP	LP	TYP	VALUE1
1	TRL1	1	3			TL	10.000000
2	STEP	4	5			SW	0.000000
3	TRL2	6	2			TL	10.000000

VALUE2	VALUE3
0.500000	0.000000
0.500000	0.800000
0.800000	0.000000

FIRST 2 PORTS ARE TREATED AS EXTERNAL PORTS

INTERCONNECTION OF VARIOUS PORTS
3 4
5 6

STARTING FREQ = 3.000000E+01GHZ, END FREQ = 4.000000E+01GHZ

BY 1.000000E+00GHZ ON A LIN SCALE

3.000000E+10 HZ

VSWR	MAGNITUDE AND PHASE OF S-PARAMETERS			
1.27517	0.12095E+00	-21.71 DEG	0.99266E+00	-3.63 DEG
1.27517	0.99266E+00	-3.63 DEG	0.12095E+00	-165.55 DEG

3.100000E+10 HZ

VSWR	MAGNITUDE AND PHASE OF S-PARAMETERS			
1.27518	0.12095E+00	-52.73 DEG	0.99266E+00	-34.61 DEG
1.27518	0.99266E+00	-34.61 DEG	0.12095E+00	-163.51 DEG

3.200000E+10 HZ

VSWR	MAGNITUDE AND PHASE OF S-PARAMETERS			
1.27518	0.12095E+00	-83.61 DEG	0.99266E+00	-65.40 DEG
1.27518	0.99266E+00	-65.40 DEG	0.12095E+00	132.81 DEG

3.300000E+10 HZ

VSWR	------MAGNITUDE AND PHASE OF S-PARAMETERS----			
1.27518	0.12095E+00	-114.35 DEG	0.99266E+00	-96.03 DEG
1.27518	0.99266E+00	-96.03 DEG	0.12095E+00	102.30 DEG

3.400000E+10 HZ

VSWR	------MAGNITUDE AND PHASE OF S-PARAMETERS----			
1.27518	0.12095E+00	-144.99 DEG	0.99266E+00	-126.51 DEG
1.27518	0.99266E+00	-126.51 DEG	0.12095E+00	71.97 DEG

3.500000E+10 HZ

VSWR	------MAGNITUDE AND PHASE OF S-PARAMETERS----			
1.27519	0.12095E+00	-175.54 DEG	0.99266E+00	-156.88 DEG
1.27519	0.99266E+00	-156.88 DEG	0.12095E+00	41.78 DEG

3.6000000E+10 HZ

VSWR	------MAGNITUDE AND PHASE OF S-PARAMETERS----			
1.27519	0.12095E+00	154.00 DEG	0.99266E+00	172.86 DEG
1.27519	0.99266E+00	172.86 DEG	0.12095E+00	11.73 DEG

3.700000E+10 HZ

VSWR	------MAGNITUDE AND PHASE OF S-PARAMETERS----			
1.27519	0.12095E+00	123.60 DEG	0.99266E+00	142.69 DEG
1.27519	0.99266E+00	142.69 DEG	0.12095E+00	-18.21 DEG

3.800000E+10 HZ

VSWR	------MAGNITUDE AND PHASE OF S-PARAMETERS----			
1.27519	0.12095E+00	93.26 DEG	0.99266E+00	112.60 DEG
1.27519	0.99266E+00	112.60 DEG	0.12095E+00	-48.05 DEG

3.900000E+10 HZ

VSWR	------MAGNITUDE AND PHASE OF S-PARAMETERS----			
1.27520	0.12095E+00	62.96 DEG	0.99266E+00	82.58 DEG
1.27520	0.99266E+00	82.58 DEG	0.12095E+00	-77.80 DEG

4.000000E+10 HZ

VSWR	------MAGNITUDE AND PHASE OF S-PARAMETERS----			
1.27520	0.12096E+00	32.70 DEG	0.99266E+00	52.61 DEG
1.27520	0.99266E+00	52.61 DEG	0.12096E+00	-107.48 DEG

APPENDIX B

```
C
C
C       MAIN PROGRAM
C       ------------
C
        SUBROUTINE FINLINE
        REAL*8 BETA,WP,A,B,SD,ER,PI,WW,DW
        COMPLEX ARG
        COMPLEX*16 C,X,S(4,4),ST
        DIMENSION SMAG(4,4),SPHA(4,4),VSWR(4)
        COMMON /FREQ/ WST,WND,DW,NSCALE
        COMMON /FREK/ BETA,WP
        COMMON /TOPO/ NCN(60),NP,NE,NPT
        COMMON /SOLN/ C(60),X(60)
        COMMON /DIMEN/ A,B,SD
        COMMON /DIELC/ ER
        COMMON /DAT/ ST,PI
        OPEN (UNIT=6,FILE='FINLINE.OUT',STATUS='NEW')
        DATA LIN,LOG /3HLIN,3HLOG/
        ST=(0.0,1.0)
        PI=4.0*DATAN(1.0D00)
        CALL FREDATA
        IOP=NPT-NP
        DO 5 J=1,IOP
        JP=NP+J
        NCN(JP)=J
        NCN(J)=JP
5       CONTINUE
        IF(NSCALE.EQ.LIN) GO TO 10
        WRITE(6,1000) WND,WST,DW
        TYPE 1000, WND,WST,DW
1000    FORMAT(1X,'WND=',30X,'WST=',50X,'DW=')
        NW=ALOG10(WND/WST)/DLOG10(DW)+1.5
        GO TO 20
10      NW=(WND-WST)/DW+1.5
20      WP=WST
        DO 23 J=1,NPT
23      C(J)=0.0
        DO 100 I=1,NW
        WW=WP/(2.0D00*PI)
        WRITE(6,30) WW
        TYPE 30, WW
        CALL FCALELMT
        CALL FSETWNC
        CALL FFACTLU
        DO 25 J=1,IOP
        JP=NP+J
        C(JP)=1.0
        CALL FFORBAK
        C(JP)=0.0
        DO 25 JL=1,IOP
        JP=NP+JL
25      S(JL,J)=X(JP)
30      FORMAT(//,15X,1PE15.6,' HZ')
```

```
      WRITE(6,45)
      TYPE *
      TYPE *,'    VSWR       ------MAGNITUDE AND PHASE OF S-PARAMETERS----'
45    FORMAT(/4X,'VSWR',6X,'------MAGNITUDE AND PHASE OF S-PARAMETERS----')
      DO 50 IP=1,IOP
      DO 50 J=1,IOP
      ARG=S(IP,J)
      SMAG(IP,J)=CABS(ARG)
      IF (SMAG(IP,J).EQ.0) THEN
              SPHA(IP,J)=0
      ELSE
              SPHA(IP,J)=ATAN2D(AIMAG(ARG),REAL(ARG))
      END IF
50    CONTINUE
      DO 53 IP=1,IOP
53    VSWR(IP)=(1.+SMAG(IP,IP))/(1.-SMAG(IP,IP))
      DO 55 IP=1,IOP
      TYPE 57, VSWR(IP),(SMAG(IP,J),SPHA(IP,J),J=1,IOP)
55    WRITE(6,57) VSWR(IP),(SMAG(IP,J),SPHA(IP,J),J=1,IOP)
57    FORMAT(1X,F10.5,2X,4(E12.5,3X,F7.2,' DEG',10X))
      IF(NSCALE.EQ.LIN) GO TO 60
      WP=WP*DW
      GO TO 100
60    WP=WP+DW
100   CONTINUE
      RETURN
      END
      BLOCK DATA
      INTEGER SA,SI,TL,SW,IS,BS,TJ,OE,RH,MT,SP,CL
      COMMON /CODE/ SA,SI,TL,SW,IS,BS,TJ,OE,RH,MT,SP,CL
      DATA SA,SI,TL,SW,IS,BS,TJ,OE,RH,MT,SP,CL /2HSA,2HSI,2HTL,2HSW,
     & 2HIS,2HBS,2HTJ,2HOE,2HRH,2HMT,2HSP,2HCL/
      END
C
C
C     SUBROUTINE TO READ INPUT DATA
C     -----------------------------
      SUBROUTINE FREDATA
      LOGICAL DISC
      INTEGER TYPE,TYP,APORT,BPORT,C,M,R,U,Y,V
      REAL*8 LENGTH,WIDTH1,WIDTH2
      REAL*8 BETA,VALUE1,VALUE2,VALUE3,PI,A,B,SD,ER,WP,DW
      COMPILE*16 ST
      INTEGER ELN,SA,SI,TL,SW,IS,BS,TJ,OE,RH,X,F,W,BBBB,SP,CL,TITLE(20
     & )
      COMMON /DAT/ ST,PI
      COMMON /DISK/ DISC
      COMMON /TOPO/ NCN(60),NP,NE,NPT
      COMMON /ELMT/ ELN(25),VALUE1(25),VALUE2(25),VALUE3(25),TYPE(25),
     & IPORT(25),JPORT(25),KPORT(25),LPORT(25),NCODE(25),V(25)
      COMMOB /CODE/ SA,SI,TL,SW,IS,BS,TJ,OE,RH,MT,SP,CL
      COMMON /FREQ/ WST,WND,DW,NSCALE
      COMMON /DIMEN/ A,B,SD
      COMMON /DIELC/ ER
      COMMON /FREK/ BETA,WP
      COMMON /PARA/ LENGTH(25),WIDTH1(25),WIDTH2(25)
      DATA NEMAX,NPMAX /25,56/
      DATA LIN,LOG,W,F,C,M,R,Y /3HLIN,3HLOG,1HW,1HF,1HO,1HM,1HR,1HY/
      TYPE *
      TYPE *,'HARD COPY IS AVALIABLE IN FILE FINLINE.OUT'
```

```
C       READ TITLE OF THE PROBLEM IN 20A4 FORMAT
        TYPE *
        TYPE *'ENTER TITLE OF THE PROBLEM (MAX 80 CHARACTERS)'
        TYPE *
        ACCEPT 10, (TITLE(IT),IT=1,20)
10      FORMAT(20A4)
        TYPE *
        TYPE *
        WRITE(6,15) (TITLE(IT),IT=1,20)
15      FORMAT(5X,20A4)
        N=1
        NP=2
C       NOW READ IN THE DESCRIPTION OF ELEMENTS
        TYPE *,'A,B,S (MM)?'
        ACCEPT *,A,B,SD
        TYPE *
        TYPE *,'ER ?'
        ACCEPT *,ER
        WRITE(6,20)A,B,SD,ER
20      FORMAT(/6X,'A =    ',F10.6,'  MM',/6X,'B =    ',F10.6,'  MM',/6X,
     &  'S =    ',F10.6,'  MM',/5X,'ER =    ',F10.6)
        WRITE(6,22)
22      FORMAT(/2X,'NE',1X,'ELN',8X,'IP',8X,'JP',8X,'KP',8X,'LP',4X,
     &  'TYP',11X,'VALUE1',14X,'VALUE2',14X,'VALUE3'/)
        DO 110 NE=1,NEMAX
        IF (U.EQ.Y) GO TO 120
        TYPE *
        TYPE *,'ELEMENT NAME (4 CHARACTERS)?'
        TYPE *
        ACCEPT 1020,ELN(NE)
1020    FORMAT(A4)
        TYPE *
        TYPE *,'FIRST PORT  :   1 OF THE 2 PORTS '
        TYPE *,'SECOND PORT :   THE 2ND PORT '
        TYPE *,'(EXTERNAL PORTS ARE TO BE NUMBERED FIRST STARTING FROM 1)'
        TYPE *,'(FOR OPEN END SECTION, NAME THE PORT IMMEDIATE TO AIR FIRST)'
        TYPE *
        TYPE *
        TYPE *'FIRST PORT NUMBER ?'
        ACCEPT *, IPORT(NE)
        TYPE *
        TYPE *,'SECOND PORT NUMBER ?'
        ACCEPT *, JPORT(NE)
        TYPE *
        TYPE *
        TYPE *,'TYPE OF COMPONENT ? CHOOSE 1 OF THE FOLLOWING'
        TYPE *
        TYPE *,'TL:   TRANSMISSION LINE SECTION'
        TYPE *,'SW:   STEP IN WIDTH'
        TYPE *,'IS:   SYMMETRICAL INDUCTIVE STRIP'
        TYPE *,'OE:   OPEN END'
        TYOE *
        ACCEPT 1000, TYPE(NE)
1000    FORMAT(A2)
        TYPE *
        TYPE *
        TYPE *,'VALUE1? CHOOSE 1 OF THE FOLLOWING'
        TYPE *,'FOR TL:   ENTER LENGTH OF TRANSMISSION LINE IN MM'
        TYPE *,'FOR SW:   TYPE 0 '
        TYPE *,'FOR IS:   ENTER LENGTH IN MM OF THE METALLIC STRIP WHICH'
```

```
      TYPE *,'                                        SEPARATES THE TWO SLOTS'
      TYPE *,'FOR OE:   TYPE 0 '
      TYPE *
      ACCEPT *,VALUE1(NE)
      TYPE *
      TYPE *
      TYPE *,'VALUE2 ? (ENTER AS SHOWN BELOW)'
      TYPE *
      TYPE *,'TL:   WIDTH(D) OF TRANSMISSION LINE IN MM'
      TYPE *,'SW:   WIDTH(W1) IN MM CONNECTED TO FIRST PORT'
      TYPE *,'IS:   SLOT WIDTH IN MM OF THE SYMMETRICAL INDUCTIVE STRIP'
      TYPE *.'OE:   TYPE 0'
      TYPE *
      ACCEPT *,VALUE2(NE)
      TYPE *
      TYPE *
      TYPE *,'VALUE3? ENTER AS SHOWN BELOW'
      TYPE *
      TYPE *,'TL:   TYPE 0'
      TYPE *,'SW:   WIDTH(W2) IN MM OF LINE AT SECOND PORT'
      TYPE *,'IS:   TYPE 0'
      TYPE *,'OE:   TYPE 0'
      TYPE *
      ACCEPT *,VALUE3(NE)
      TYPE *
      TYPE *
      TYPE *
      TYPE *,'DATA INPUT OF COMPONENTS FINISHED?   (Y/N)'
      ACCEPT 16, U
16    FORMAT(A1)
      TYP=TYPE(NE)
      LENGTH(NE)=VALUE1(NE)
      WIDTH1(NE)=VALUE2(NE)
      WIDTH2(NE)=VALUE3(NE)
      CALL FELCODE(TYP,NC)
      NCODE(NE)=NC
      IF(NP.LT.IPORT(NE)) NP=IPORT(NE)
      GO TO (40,40,40,40,40,40,40,60,91,40,90,96) ,NC
40    IF(NP.LT.JPORT(NE)) NP=JPORT(NE)
      WRITE(6,45) NE,ELN(NE),IPORT(NE),JPORT(NE),TYP,VALUE1(NE),VALUE2(NE
     &  ),VALUE3(NE),V(NE)
45    FORMAT(1X,I3,1X,A4,4X,I5,5X,I5,25X,A2,8X,F10.6,10X,F10.6,10X,F10.6
     &  ,3X,A1)
      GO TO 100
60    WRITE(6,70) NE,ELN(NE),IPORT(NE),JPORT(NE),KPORT(NE),TYP,VALUE1(NE)
     &  ,VALUE2(NE)
70    FORMAT(1X,I3,A4,5X,I5,5X,I5,5X,I5,15X,A2,5X,E15.6,5X,E15.6)
      IF(NP.LT.JPORT(NE)) NP=JPORT(NE)
      IF(NP.LT.KPORT(NE)) NP=KPORT(NE)
      GO TO 100
85    FORMAT(1X,I3,A4,5X,I5,35X,A2,5X,E15.6)
91    IF(LPORT(NE).NE.0) GO TO 97
      IF(KPORT(NE).EQ.0) GO TO 93
      WRITE(6,92) NE,ELN(NE),IPORT(NE),JPORT(NE),KPORT(NE),TYP
92    FORMAT(1X,I3,A4,5X,I5,5X,I5,5X,I5,15X,A2)
      IF(NP.LT.JPORT(NE)) NP=JPORT(NE)
      IF(NP.LT.KPORT(NE)) NP=KPORT(NE)
      GO TO 100
93    IF(JPORT(NE).EQ.0) GO TO 101
      WRITE(6,94) NE,ELN(NE),IPORT(NE),JPORT(NE),TYP
```

```
94      FORMAT(1X,I3,A4,5X,I5,5X,I5,25X,A2)
        IF(NP.LT.JPORT(NE)) NP=JPORT(NE)
        GO TO 100
101     WRITE(6,102) NE,ELN(NE),IPORT(NE),TYP
102     FORMAT(1X,I3,A4,5X,I5,35X,A2)
        GO TO 100
97      WRITE(6,99) NE,ELN(NE),IPORT(NE),JPORT(NE),KPORT(NE),LPORT(NE),TYP
99      FORMAT(1X,I3,A4,5X,I5,5X,I5,5X,I5,5X,I5,5X,A2)
        IF(NP.LT.JPORT(NE)) NP=JPORT(NE)
        IF(NP.LT.KPORT(NE)) NP=KPORT(NE)
        IF(NP.LT.LPORT(NE)) NP=LPORT(NE)
        GO TO 100
90      WRITE(6,95) NE,ELN(NE),IPORT(NE),TYP,VALUE1(NE)
95      FORMAT(1X,I3,A4,5X,I5,35X,A2,5X,E15.6)
        GO TO 100
96      WRITE(6,98) NE,ELN(NE),IPORT(NE),JPORT(NE),KPORT(NE),LPORT(NE),TYP,
     &  VALUE1(NE),VALUE2(NE),V(NE)
98      FORMAT(1X,I3,A4,5X,I5,5X,I5,5X,I5,5X,I5,5X,A2,5X,E15.6,5X,
     &  E15.6,1X,A1)
        IF(NP.LT.JPORT(NE)) NP=JPORT(NE)
        IF(NP.LT.KPORT(NE)) NP=KPORT(NE)
        IF(NP.LT.LPORT(NE)) NP=LPORT(NE)
100     IF(NP.LE.NPMAX) GO TO 110
        WRITE(6,105)
        TYPE *,'NUMBER OF PORTS EXCEEDS NPMAX.STOP.'
105     FORMAT(5X,'NUMBER OF PORTS EXCEEDS NPMAX.STOP.')
        STOP
110     CONTINUE
        WRITE(6,115)
        TYPE *,'NUMBER OF ELEMENTS EXCEEDS NEMAX.STOP.'
115     FORMAT(5X,'NUMBER OF ELEMENTS EXCEEDS NEMAX.STOP.')
        STOP
120     NE=NE-1
        TYPE *,'NUMBER OF EXTERNAL PORTS ?'
        TYPE *
        ACCEPT *, IOP
        WRITE(6,127) IOP
125     FORMAT(I1)
127     FORMAT(//,5X,'FIRST',I2,' PORTS ARE TREATED AS EXTERNAL PORTS')
        NPT=NP+IOP
C       NOW READ IN INTERCONNECTIONS OF VARIOUS PORTS
        WRITE(6,128)
128     FORMAT(/2X,'INTERCONNECTION OF VARIOUS PORTS')
        NJ=(NP-IOP)/2
        DO 140 I=1,NJ
        TYPE *,'ENTER THE INTERCONNECTION BETWEEN VARIOUS PORTS'
        TYPE *,'2 AT A TIME'
        TYPE *
        ACCEPT *,APORT,BPORT
        NCN(APORT)=BPORT
        NCN(BPORT)=APORT
140     WRITE(6,145) APORT,BPORT
145     FORMAT(15X,I5,5X,I5)
        TYPE *
        TYPE *,'STARTING FREQUENCY ? (IN GHZ OR IN RAD/S)'
        ACCEPT *,WST
        TYPE *
        TYPE *,'END FREQUENCY ? (IN GHZ OR IN RAD/S)'
        ACCEPT *,WND
        TYPE *
```

```
      TYPE *,'FREQUENCY INCREMENT ? (FOR LINEAR SCALE)'
      TYPE *,'FACTOR ? (FOR LOG SCALE)'
      TYPE *
      ACCEPT *,DW
      TTPE *
      TYPE *,'STARTING & END FREQUENCIES IN GHZ OR RAD/S ? (F/X)'
      ACCEPT 16, X
      TYPE *
      TYPE *,'LINEAR / LOG SCALE ? (LIN/LOG)'
      ACCEPT 1010, NSCALE
1010  FORMAT(A3)
      IF(X.EQ.F) GO TO 170
      WRITE(6,160) WST,WND,DW,NSCALE
160   FORMAT(/1X,'STARTING FREQ =',1PE15.6,'RAD/SEC,END FREQ =',
     & 1PE15.6,'RSD/SEC',//5X,' BY',1PE15.6,'   ON A  ',A3,'  SCALE')
      GO TO 190
170   WRITE(6,180) WST,WND,DW,NSCALE
180   FORMAT(/1X,'STARTING FREQ =',1PE15.6,'GHZ,END FREQ =',1PE15.6,
     & 'GHZ',//5X,'BY',1PE15.6,'GHZ   ON A  ',A3,'  SCALE')
      WND=WND*0.1D10*PI*2.0D00
      WST=WST*0.1D10*PI*2.0D00
      IF(NSCALE.EQ.LOG) GO TO 190
      DW=DW*0.1D10*PI*2.0D00
190   IF(J.EQ.Y) GO TO 210
      DISC=.FALSE.
      RETURN
210   DISC=.TRUE.
      RETURN
      END
C
      SUBROUTINE FELCODE(TYP,NC)
      INTEGER TYP,SA,SI,TL,SW,IS,BS,TJ,OE,RH,MT,SP,CL
      COMMON /CODE/ SA,SI,TL,SW,IS,BS,TJ,OE,RH,MT,SP,CL
      NC=0
      IF(TYP.EQ.TL)NC=3
      IF(TYP.EQ.SW)NC=4
      IF(TYP.EQ.IS)NC=5
      IF(NC.NE.0) RETURN
      WRITE(6,10)
      TYPE *,'  INCORRECT CODE FOR ELEMENT TYPE'
      TYPE *,'PLEASE CHECK INPUT DATA.STOP.'
10    FORMAT('  INCORRECT CODE FOR ELEMENT TYPE'/'PLEASE CHECK INPUT DATA.
     & STOP.')
      STOP
      END
C
C     SUBROUTINE TO SET MATRIX W
C     --------------------------
      SUBROUTINE FSETWNC
      INTEGER ELN,TYPE,V
      REAL*8 BETA,VALUE1,VALUE2,VALUE3,VAL1,VAL2,VAL3,WP
      COMPLEX*16 S,W
      COMMON /MTRX/ W(60,60)
      COMMON /ELMT/ ELN(25),VALUE1(25),VALUE2(25),VALUE3(25),TYPE(25),
     & IPORT(25),JPORT(25),KPORT(25),LPORT(25),NCODE(25),V(25)
      COMMON /TOPO/ NCN(60),NP,NE,NPT
      COMMON /EMTX/S(4,4),VAL1,VAL2,VAL3
      COMMON /SETT/IP,JP,KP,LP
      COMMON/FREK/ BETA,WP
      DO 10 I=1,NPT
```

```
      DO 10 J=1,NPT
10    W(I,J)=0.0
      DO 20 I=1,NPT
      J=NCN(I)
20    W(I,J)=1.0
      DO 150 I=1,NE
      NC=NCODE(I)
      IP=IPORT(I)
      VAL1=VALUE1(I)
      VAL2=VALUE2(I)
      VAL3=VALUE3(I)
      GO TO (60,70,80),NC
60    CALL FLINESC
      CALL FSETOPS
      GO TO 150
70    CALL FSTEPSC
      CALL FSETUPS
      GO TO 150
80    CALL FINDUCSC
      CALL FSETUPS
      GO TO 150
150   CONTINUE
      RETURN
      END
C
C     SUBROUTINE FOR L-U FACTORIZATION OF W-MATRIX
C     ---------------------------------------------
      SUBROUTINE FFACTLU
      COMPLEX*16 W
      COMMON /TOPO/ NCN(60),NP,NE,NPT
      COMMON /MTRX/ W(60,60)
      NP1=NPT-1
      DO 20 L=1,NP1
      L1=L+1
      LPR=NCN(L)
      DO 10 I=L1,NPT
      IPR=NCN(I)
10    W(L,IPR)=W(L,IPR)/W(L,LPR)
      DO 20 I=L1,NPT
      DO 20 J=L1,NPT
      JPR=NCN(J)
20    W(I,JPR)=W(I,JPR)-W(I,LPR)*W(L,JPR)
      RETURN
      END
C
      SUBROUTINE FSETUPS
      REAL*8 VAL1,VAL2,VAL3
      COMPLEX*16 S,W
      COMMON /EMTX/ S(4,4),VAL1,VAL2,VAL3
      COMMON /MTRX/ W(60,60)
      COMMON /SETT/ IP,JP,KP,LP
      W(IP,IP)=-S(1,1)
      W(IP,JP)=-S(1,2)
      W(JP,IP)=-S(2,1)
      W(JP,JP)=-S(2,2)
      RETURN
      END
C
      SUBROUTINE FFORBAK
      COMPLEX*16 X,W,C,R
```

```
      COMMON /TOPO/ NCN(60),NP,NE,NPT
      COMMON /MTRX/ W(60,60)
      COMMON /SOLN/ C(60),X(60)
C     FORWARD ELIMINATION
      I=NCN(1)
      X(I)=C(1)/W(1,I)
      DO 20 I=2,NPT
      R=0.0
      IPR=NCN(I)
      I1=I-1
      DO 10 L=1,I1
      LPR=NCN(L)
10    R=R+W(I,LPR)*X(LPR)
20    X(IPR)=(C(I)-R)/W(I,IPR)
C     BACK SUBSTITUTION
      NP1=NPT-1
      DO 40 K=1,NP1
      I=NPT-K
      R=0.0
      IPR=NCN(I)
      I1=I+1
      DO 30 L=I1,NPT
      LPR=NCN(L)
30    R=R+W(I,LPR)*X(LPR)
40    X(IPR)=X(IPR)-R
      RETURN
      END
C
C     SUBROUTINE TO CALCUALTE EFFECTIVE DIELECTRIC CONSTANT ERE
C     ---------------------------------------------------------
      SUBROUTINE FEREFF(D,ERE)
      REAL*8 BETA,ERE,D,A,B,SD,ER,PI,WP
      COMPLEX*16 ST
      COMMON /DIMEN/ A,B,SD
      COMMON /DIELC/ ER
      COMMON /DAT/ ST,PI
      COMMON /FREK/ BETA,WP
      A1=0.4021*(DLOG(SD/A))**2-0.7685*DLOG(A/SD)+0.3972
      B1=2.42*DSIN(0.556*DLOG(A/SD))
      ERE=1+SD/A*(A1*DLOG(1/DSIN(PI/2*D/B))+B1)*(ER-1)
      RETURN
      END
C
C     TO CALCULATE THE CHARACTERISTICS OF DIFFERENT COMPONENTS
C     -------------------------------------------------------
      SUBROUTINE FCALELMT
      INTEGER C,R,W,U,V
      REAL*8 LENGTH,L,PI,WP,WIDTH1,WIDTH2,W1,W2,SQEFF_AIR,SQLFF_DIE
      REAL*8 BETA,INDUC,NORSUS,ELEC_LEN,VALUE1,VALUE2,VALUE3,Z,ZRATIO
      COMPLEX*16 ST
      COMMON /DAT/ ST,PI
      COMMON /DISK/ DISC
      COMMON /FREK/ BETA,WP
      COMMON /TOPO/ NCN(60),NP,NE,NPT
      COMMON/ ELMT/ ELN(25),VALUE1(25),VALUE2(25),VALUE3(25),TYPE(25),
     & IPORT(25),JPORT(25),KPORT(25),LPORT(25),NCODE(25),V(25)
      COMMON /PARA/ LENGTH(25),WIDTH1(25),WIDTH2(25)
      DATA W,C,R /1HW,1HC,1HR/
C
      DO 100 I=1,NE
```

```
      NC=NCODE(I)
      U=V(I)
      L=LENGTH(I)
      W1=WIDTH1(I)
      W2=WIDTH2(I)
      CALL FIMPFWD(W1,Z)
      VALUE1(I)=L*BETA
      VALUE2(I)=Z
      IF (NC.EQ.3) GO TO 100
      IF (NC.EQ.5) GO TO 27
      CALL FSTEPCAL(W1,W2,Z,ZRATIO,INDUC)
      VALUE2(I)=ZRATIO
      VALUE3(I)=INDUC
      GO TO 100
27    CALL FINDUCAL(L,W1,NORSUS,ELEC_LEN)
      VALUE1(I)=NORSUS
      VALUE2(I)=ELEC_LEN
      GO TO 100
100   CONTINUE
      RETURN
      END
C
C     SUBROUTINE TO FIND CH.IMPEDANCE AND GUIDED WAVELENGTH FROM DIMENSION
C     ---------------------------------------------------------------------
C     OF CONDUCTION LINE
C     ------------------
      SUBROUTINE FIMPFWD(D,ZOVP)
      REAL*8 BETA,K1,K2,KC,KE,P,Q1,QF,R,S0,S1,V,W,X1,X2,XCR,XCF,XG,XW,ZOVP
      REAL*8 A,B,D,SD,ER,WP,PI
      COMPLEX*16 ST
      COMMON /FREQ/ WST,WND,DW,NSCALE
      COMMON /FREK/ BETA,WP
      COMMON /DIMEN/ A,B,SD
      COMMON /DIELC/ ER
      COMMON /DAT/ ST,PI
C
C     TO CALCULATE THE GUIDED WAVELENGTH
C
      CALL FEREFF(D,KC)
      XCR=2*A*DSQRT(1+(4/PI)*(1+0.2*DSQRT(B/A))*(B/A)*DLOG(1/DSIN(PI/2)*
     &  (D/B))))
      XW=2*PI*0.3E09*1000/WP
      XCF=XCR*DSQRT(KC)
      QF=(KC-1)/(ER-1)
      S0=DSQRT(0.0666+0.0466*QF**2+0.015*QF**4-0.00137*QF**6)+QF/(PI*PI)
      S1=DEXP(1./3*DLOG(S0))
      V=-2*QF/(PI*PI)+S1**3
      W=-DEXP(1./3*DLOG(V))
      P=W+S1+QF/3
      K1=1+PI*PI/12*P*(3-2*P)*(ER-1)
      X1=XCR*PI*DSQRT(P*(3-2*P)*(ER-1)/12)
      KE=KC+(K1-KC)/(B/X1-B/XCF)*(B/XW-B/XCF)
      XG=XW/DSQRT(KE-(XW/XCR)**2)
      BETA=2*PI/XG
C
C     TO CALCULATE THE CHARACTERISTIC IMPEDANCE
C
      X2=DLOG(1/DSIN(PI/2*D/B))
      IF(D/B.GT.0.3D00 GO TO 10
      K2=0.17*(B/XW)+0.0098
```

```
      Q1=0.138*(B/XW)+0.873
      GO TO 20
10    R=0.0775*(DLOG(A/SD))**2-0.668*(DLOG(A/SD))+1.262
      K2=-0.763*(B/XW)**2+0.58*(B/XW)+R
      Qi=0.372*(B/XW)+0.914
20    ZOVP=120*PI*PI*(K2*X2+Q1)*(2*B/A)/((0.385*X2+1.762)**2*(XW/XG))
      RETURN
      END
C
C     SUBROUTINE TO CALCULATE THE IMPEDANCE RATIO AND NORMALIZED INDUCTANCE
C     ---------------------------------------------------------------------
      SUBROUTINE FSTEPCAL(W1,W2,Z1,ZRATIO,INDUC)
      REAL*8 BETA,INDUC,W,ZR1,ZR2,ZRATIO,W1,W2,Z1,WP
      COMMON /FREK/ BETA,WP
      W=W2/W1
      IF((W.GT.8.8D00).AND.(W.LE.13.6D00)) GO TO 10
      ZR1=0.7025+1.19*W1
      ZR2=0.7025+1.19*W2
      IF (W1.EQ.0.25D00) ZR1=1.0D00
      GO TO 20
10    ZR1=1.879+0.6554*W1
      ZR2=1.879+0.6554*W2
      IF (W1.EQ.0.25D00) ZR1=1.0D00
20    ZRATIO=ZR2/ZR1
      INDUC=WP*(19.14-31.275*W+14.56*W**2-0.5014*W**3)*0.1D-11/Z1
      RETURN
      END
C
C     SUBROUTINE TO CALCULATE THE NORMALIZED SUSCEPTANCE AND ELECTRICAL
C     LENGTH OF A SYMMETRICAL INDUCTIVE STRIP
C     ---------------------------------------
      SUBROUTINE FINDUCAL(S,D,NORSUS,ELEC_LEN)
      COMPLEX*16 ST
      REAL*8 NORSUS,NOR_LEN,ELEC_LEN,S,D,BETA,WP,A,B,SD,PI
      REAL*8 XW,XA1,XA2,XB1,XB2,XC1,XC2,XD1,XD2,XE1,XE2,YA,YB,YC,YD,YE
      COMMON /FREK/ BETA,WP
      COMMON /DIMEN/ A,B,SD
      COMMON /DAT/ ST,PI
      XW=2*PI*0.3D09*1000/WP
      NORSUS=(2.778+39.26*(S/B)-33.43*(S/B)**2+111.4*(S/B)**3)*(4.156-
     & 14.472*(B/XW)+15.218*(B/XW)**2)*(0.6046+0.05926*(B/D)-0.001224*
     & (B/D)**2)
      IF ((S/B.GT.0.1D00).AND.(S/B.LE.0.4D00)) GO TO 10
      XA1=-0.09806+12.464*(D/B)-29.432*(D/B)**2
      XA2=1.185+13.559*(D/B)-17.958*(D/B)**2
      XB1=0
      XB2=0.62135+2.8438*(D/B)+1.4831*(D/B)**2
      YA=(XA2-XA1)/0.203*(B/XW-0.473)+XA2
      YB=(XB2-XB1)/0.203*(B/XW-0.473)+XB2
      NOR_LEN=0.2995*YA*(S/B)-3.562*YB*(S/B)**2
      GO TO 30
C
10    XA1=-3.70847+58.853*(D/B)-169.48*(D/B)**2
      XA2=-55.557+716.52*(D/B)-2505*(D/B)**2
      XB1=-0.4982+17.445*(D/B)-43.674*(D/B)**2
      XB2=-1.675+45.422*(D/B)-131.98*(D/B)**2
      XC1=15.855-183.46*(D/B)+516.99*(D/B)**2
      XC2=58.531-1141.5*(D/B)+3447.4*(D/B)**2
      XD1=1.1443-2.4656*(D/B)+10.487*(D/B)**2
      XD2=6.9035-127.76*(D/B)+389.87*(D/B)**2
```

```
      XE1=0.19323+9.1992*(D/B)-21.961*(D/B)**2
      XE2=4.9952-90.588*(D/B)+277.26*(D/B)**2
      YA=(XA2-XA1)/0.203*(B/XW-0.473)+XA2
      YB=(XB2-XB1)/0.203*(B/XW-0.473)+XB2
      XC=(XC2-XC1)/0.203*(B/XW-0.473)+XC2
      YD=(XD2-XD1)/0.203*(B/XW-0.473)+XD2
      YE=(XE2-XE1)/0.203*(B/XW-0.473)+XE2
      NOR_LEN=-0.0004874*YA+0.3179*YB*(S/B)+0.0925*YC*(S/B)**2-2.563*YD
     &*(S/B)**3+3.885*YB*(S/B)**4
C
30    ELCE_LEN=B*NOR_LEN
      RETURN
      END
C
CC    SUBROUTINE TO CALCULATE S-MATRIX FOR TRANSMISSION LINE
C     ------------------------------------------------------
      SUBROUTINE FLINESC
      REAL*8 BETA,VAL1,VAL2,VAL3,PI,WP
      COMPLEX*16 S,ST
      COMMON /EMTX/ S(4,4),VAL1,VAL2,VAL3
      COMMON /DAT/ ST,PI
      COMMON /FREK/ BETA,WP
      S(1,1)=0.0
      S(1,2)=DCOS(VAL1)-ST*DSIN(VAL1)
      S(2,1)=S(1,2)
      S(2,2)=0.0
      RETURN
      END
C
CC    SUBROUTINE TO CALCULATE S-MATRIX FOR STEP DISCONTINUITY
C     -------------------------------------------------------
      SUBROUTINE FSTEPSC
      LOGICAL DISC
      REAL*8 BETA,VAL1,VAL2,VAL3,PI,WP
      COMPLEX*16 S,ST
      COMMON /EMTX/ S(4,4),VAL1,VAL2,VAL3
      COMMON /DISK/ DISC
      COMMON /DAT/ ST,PI
      COMMON /FREK/ BETA,WP
C
      S(1,1)=(VAL2-1+ST*VAL3)/(VAL2+1+ST*VAL3)
      S(1,2)=2*DSQRT(VAL2)/(VAL2+1+ST*VAL3)
      S(2,1)=S(1,2)
      S(2,2)=-(VAL2-1-ST*VAL3)/(VAL2+1+ST*VAL3)
      RETURN
      END
C
CC    SUBROUTINE TO CALCULATE S-MATRIX FOR SYMMETRICAL INDUCTIVE STRIP
C     ----------------------------------------------------------------
      SUBROUTINE FINDUCSC
      REAL*8 VAL1,VAL2,VAL3,PI,BETA,WP
      COMPLEX*16 S,DENOM,ST
      COMMON /EMTX/ S(4,4),VAL1,VAL2,VAL3
      COMMON /DAT/ ST,PI
      COMMON /FREK/ BETA,WP
C
      DENOM=(2+ST*VAL1)*CDEXP(2*ST*BETA*VAL2)
      S(1,1)=-(ST*VAL1)/DENOM
      S(1,2)=2/DENOM
      S(2,1)=S(1,2)
```

```
S(2,2)=S(1,1)
RETURN
END
```

APPENDIX C

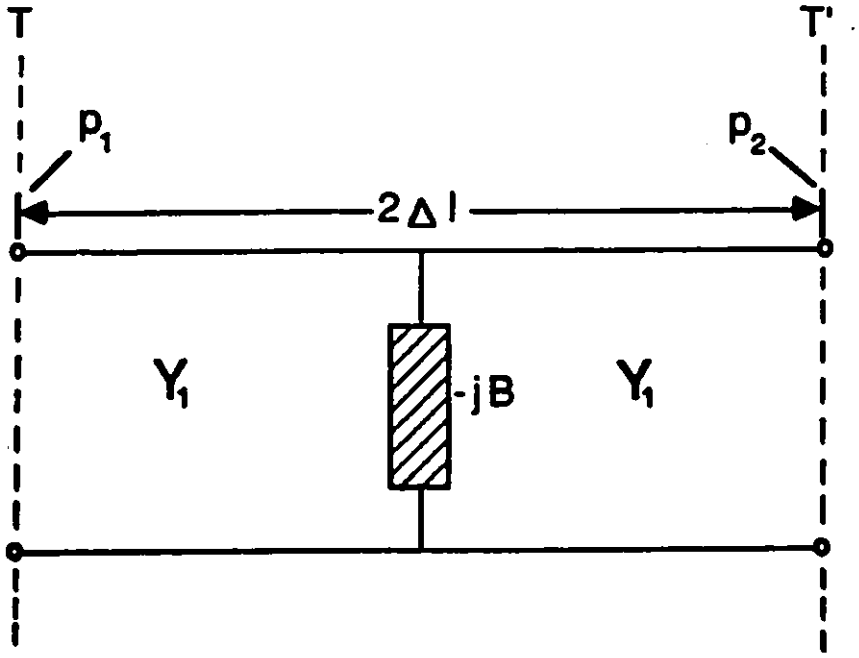

The above equivalent circuit is composed of three cascaded two-port networks: two transmission lines of length Δl cascaded to a shunt admittance.

The ABCD matrix of a transmission line is $\begin{bmatrix} cosh(\gamma\Delta l) & \frac{1}{Y_1}sinh(\gamma\Delta l) \\ Y_1 sinh(\gamma\Delta l) & cosh(\gamma\Delta l) \end{bmatrix}$.

The ABCD matrix of a shunt admittance is $\begin{bmatrix} 1 & 0 \\ -jB & 1 \end{bmatrix}$.

The overall ABCD matrix is obtained by multiplying the three matrices together.

$$\begin{bmatrix} A & B \\ C & D \end{bmatrix} = \begin{bmatrix} cosh(\gamma\Delta l) & \frac{1}{Y_1}sinh(\gamma\Delta l) \\ Y_1 sinh(\gamma\Delta l) & cosh(\gamma\Delta l) \end{bmatrix} \times \begin{bmatrix} 1 & 0 \\ -jB & 1 \end{bmatrix} \times \begin{bmatrix} cosh(\gamma\Delta l) & \frac{1}{Y_1}sinh(\gamma\Delta l) \\ Y_1 sinh(\gamma\Delta l) & cosh(\gamma\Delta l) \end{bmatrix}$$

$$S_{11} = \frac{\frac{A}{Y_1} + B - \frac{C}{Y_1^2} - \frac{D}{Y_1}}{\frac{A}{Y_1} + B + \frac{C}{Y_1^2} + \frac{D}{Y_1}}$$

$$S_{12} = \frac{2(AD - BC)/Y_1}{\frac{A}{Y_1} + B + \frac{C}{Y_1^2} + \frac{D}{Y_1}}$$

By simplifying the expressions for S_{11} and S_{12}, we obtain

$$S_{11} = \frac{-j\frac{-B}{Y_1}}{(2 + j\frac{-B}{Y_1})(cosh(\gamma\Delta\ell) + sinh(\gamma\Delta\ell))^2} \tag{4.1}$$

$$S_{12} = \frac{2}{(2 + j\frac{-B}{Y_1})(cosh(\gamma\Delta\ell) + sinh(\gamma\Delta\ell))^2} \tag{4.2}$$

REFERENCES

[1] P.J. Meier, "Integrated Fin-Line Millimeter Components", *IEEE Trans., Microwave Theory and Techniques*, vol. MTT-22, pp.1209-1216, 1974.

[2] H. Hofmann, "Calculation of Quasi-Planar Lines for MM-Wave Application", *1977 IEEE MTT-S Int. Microwave Symp. Dig.*, San Diego, Ca., USA, pp.381-383.

[3] G. Begemann, "An X-band Balanced Fin-Line Mixer", *1978 IEEE MTT-S Int. Microwave Symp. Dig.*, Ottawa, Ont., Canada, pp.24-26.

[4] R. Knoechel, "Design and Performance of Microwave Oscillators in Integrated Fin-Line Technique", *Microwave, Optics and Acoustics*, vol. 3, pp.115-120, 1979.

[5] L.D. Cohen and P.J. Meier, "Advances in E-plane Printed Millimeter-Wave Circuits", *1978 IEEE MTT-S Int. Microwave Symp. Dig.*, Ottawa, Ont., Canada, pp.27-29.

[6] A.M.K. Saad and G. Begemann, "Electrical Performance of Finlines of Various Configurations", *IEE J. of Microwaves, Optics and Acoustics*, vol. 1, pp.81-88, 1977.

[7] C. Chang and T. Itoh, "Spectral Domain Analysis of Dominant and Higher Order Modes in Fin-Lines", *1979 IEEE MTT-S Int. Microwave Symp. Dig.*, Orlando, Florida, USA, pp.344-346.

[8] W.J.R. Hoefer, "Fin Line Design Made Easy", *1978 IEEE MTT-S Int. Microwave Symp. Dig.*, Ottawa, Ont., Canada, pp.471.

[9] P. Pramanick and P. Bhartia, "Accurate Analysis Equations and Synthesis Technique for Unilateral Finlines", *IEEE Trans., Microwave Theory and Techniques*, vol. MTT-33, pp.24-30, 1985.

[10] M. Helard, J. Citerne, O. Picon and V. Fouad-Hanna, "Solution of Fin-Line Discontinuities Through the Identification of its First Four Higher Order Modes", *1983 IEEE MTT-S Int. Microwave Symp. Dig.*, pp.387-389.

[11] N.H.L. Koster and R.H. Jansen, "Some New Results on the Equivalent Circuit Parameters of the Inductive Strip Discontinuity in Unilateral Fin Lines", *AEU, Arch. Electron*

Uebertragungs tech, 1981, vol. 35, pp.497-499.

[12] R. Sorrentino and T. Itoh, "Transverse Resonance Analysis of Finline Discontinuities", *IEEE Trans., Microwave Theory and Techniques*, vol. MTT-32, pp.1633-1638, 1984.

[13] A.M.K. Saad and K. Schuenemann, "A Simple Method for Analyzing Fin-Line Structures", *IEEE Trans., Microwave Theory and Techniques*, vol. MTT-26, pp.1002-1007, 1978.

[14] H. El Hennawy and K. Schuenemann, "Analysis of Fin-Line Discontinuities", *Proc. of the 9th European Microwave Conf.*, Brighton, England, 1979, pp.448-452.

[15] M. Helard, J. Citerne, O. Picon and V. Fouad-Hanna, "Exact Calculations of Scattering Parameters of a Step Slot Width Discontinuity in a Unilateral Fin-Line", *Electron. Lett.*, pp.537-539, July 1983.

[16] L.P. Schmidt, AEG-Telefunken, Ulm, private communications.

[17] E. Pic and W.J.R. Hoefer, "Experimental Characterization of Fin Line Discontinuities using Resonant Techniques", *1981 IEEE MTT-S Int. Microwave Symp. Dig.*, Los Angeles, CA., USA, pp.108-110.

[18] H. Hofmann, H. Meinel and B. Adelseck, "New Integrated MM-Wave Components using Fin-Lines", *1978 IEEE MTT-S Int. Microwave Symp. Dig.*, Ottawa, Ont., Canada, pp.21-23.

[19] H. El Hennawy and K. Schuenemann, "Impedance Transformation in Fin Lines", *IEE Proc. H*, vol. 129, pp.342-350, 1982.

[20] K.C. Gupta, R. Garg and R. Chadha, "Computer-Aided Design of Microwave Circuits", Artech House, Dedham, Ma., 1981.

[21] R.E. Collin, "Foundations for Microwave Engineering", *McGraw-Hill*, Higtstown, NJ, USA, 1966.

[22] M. Helard, J. Citerne, O. Picon and V. Fouad-Hanna, "Theoretical and Experimental Investigation of Finline Discontinuities", *IEEE Trans., Microwave Theory and Techniques*, vol. MTT-33, pp.994-1003, 1985.

[23] R.E. Collin, "Field Theory of Guided Waves", McGraw-Hill, Highstown, NJ, USA, 1960.

[24] K.J. Webb and R. Mittra, "Solution of the Finline Step-Discontinuity Problem Using the Generalized Variational Technique", *IEEE Trans., Microwave Theory and Techniques*, vol. MTT-33, pp.1004-1010, 1985.

[25] Y.L. Tsui and W.J.R. Hoefer, "Empirical Formulae for the parameters of Impedance Steps

and Inductive Strips in Finline", *IEEE Montech'86 Digest*, Montreal, Que., Canada, pp.36-38.

[26] R.K. Hoffmann, "Handbook of Microwave Integrated Circuits", pp.136-137, Artech House, Norwood, Ma., 1987.

[27] J.B. Knorr and J.C. Deal, "Scattering Coefficients of an Inductive Strips in a Finline: Theory and Experiment", *IEEE Trans. Microwave Theory and Techniques*, vol. MTT-33, pp.1011-1017, Oct. 1985.

[28] A. Biswas and B. Bhat, "Accurate Characterization on an Inductive Strip in Finline", *IEEE Trans. Microwave Theory and Techniques*, vol. 36, pp.1233-1238, Aug. 1988.

[29] K.C. Gupta, R. Garg and I.J. Bahl, "Microstrip Lines and Slotlines", Artech House, Dedham, Ma., 1979.